

Appendix

By Natasha B. Carr, Kirk R. Sherrill, Gordon Reese, Annika K. Walters, Andrea Ray, James Littell, Steven L. Garman, Catherine S. Jarnevich, Lucy Burris, and Jena R. Hickey

Contents

Introduction.....	832
Distribution Mapping of Communities and Species.....	832
Terrestrial Ecological Community Distribution Maps.....	832
Plant Species Distribution Maps.....	837
Aspen Forests and Woodlands	837
Aquatic Ecological Community Distribution Maps	838
Riparian Areas.....	838
Species Distribution Models.....	838
Greater Sage-Grouse Habitat Model	838
Species Distribution Modeling using MaxEnt.....	842
General Approach.....	842
Spadefoot Assemblage.....	845
Golden Eagle	846
Ferruginous Hawk.....	846
Pygmy Rabbit	847
Species Occupancy Modeling for Sagebrush-Obligate Songbirds	848
Brewer’s Sparrow	848
Sagebrush Sparrow	850
Sage Thrasher	850
Change Agents.....	851
Development.....	851
Terrestrial Development Index	851
Selection of Moving-Window Size.....	852
Selection of Terrestrial Development Index Breakpoints	855
Comparison of the Terrestrial Development Index to Other Similar Approaches.....	855
Validation of Terrestrial Development Index	856
Aquatic Development Index.....	858
Invasive Species	863
Landscape Structure: Terrestrial Structural Connectivity Analysis	865
Integrated Management Questions.....	870
Wildland Fire	877
Climate Analysis.....	880
Current Climate—Observations and Analysis	880
Future Climate—Projections Methods and Datasets.....	881

Choice of CMIP3 Generation of Models.....	881
The Global Context.....	882
Downscaling Products and Methods.....	882
Comparison and Strengths and Weaknesses of Downscaling Products.....	885
Visualizing the Climates in the Downscaled Global Climate Models.....	887
Hydroclimate.....	890
Data Gaps and Uncertainty.....	890
References Cited.....	891

Figures

A-1. Patch size of potential greater sage-grouse habitat using a probability threshold of 0.49 and 0.25 for the baseline general-use habitat model.....	841
A-2. Structural connectivity of relatively undeveloped greater sage-grouse habitat as a function of interpatch distance at two thresholds in probability of occurrence.....	842
A-3. Evaluation of optimal window size for calculating the Terrestrial Development Index.....	853
A-4. Terrestrial Development Index scores for several sizes of moving windows.....	854
A-5. The relationship between the predicted probability of occurrence for greater sage-grouse and the Terrestrial Development Index.....	857
A-6. Diagram of the local and upstream contributing area used for calculating the overall Aquatic Development Index.....	859
A-7. Examples of nested catchments and watersheds.....	860
A-8. Aquatic Development Index.....	862
A-9. Correspondence between the Wyoming Stream Integrity Index and upstream Aquatic Development Index scores.....	863
A-10. Connectivity analysis for determining local, landscape, and regional levels of structural connectivity for sagebrush steppe, desert shrublands, foothill shrublands and woodlands, and mountain forests and alpine zones.....	866
A-11. Connectivity analysis for determining local, landscape, and regional levels of structural connectivity for wetlands, aspen, five-needle pine forests and woodlands, and juniper woodlands.....	867
A-12. Connectivity analysis for determining local, landscape, and regional levels of structural connectivity for greater sage-grouse, golden eagle, ferruginous hawk, and sagebrush-obligate birds.....	868
A-13. Connectivity analysis for determining local, landscape, and regional levels of structural connectivity for pygmy rabbit, mule deer crucial winter range, and spadefoot assemblage.....	869
A-14. Annual average temperature around 2030 shown for downscaled products at two resolutions....	886
A-15. Range of projected futures in global climate models for the Wind River Range.....	889

Tables

A-1.	Cross walk used to classify LANDFIRE Existing Vegetation Types as ecological communities...	833
A-2.	Explanatory variables used in the sage-grouse baseline general-use model	839
A-3.	Omission error for lek occurrence as a function of probability threshold for the baseline greater sage-grouse general-use habitat model	839
A-4.	Environmental variables evaluated for contribution to species distribution models.....	843
A-5.	Data sources and number of occurrences considered for MaxEnt modeling of potential habitat for Conservation Elements	845
A-6.	Variables, data sources, and percent contribution to the top MaxEnt model for the spadefoot assemblage	845
A-7.	Variables, data sources, and percent contribution to top MaxEnt model for golden eagle nesting habitat.....	846
A-8.	Variables, data sources, and percent contribution to top MaxEnt model for ferruginous hawk.....	847
A-9.	Variables, data sources, and percent contribution to top MaxEnt model for pygmy rabbit habitat.....	848
A-10.	Variables and logit link function parameters for the Brewer’s sparrow occupancy model.....	849
A-11.	Variables and logit link function parameters for the sagebrush sparrow occupancy model	850
A-12.	Variables and logit link function parameters for the sage thrasher occupancy model.....	851
A-13.	Surface disturbance buffers used for quantifying the surface disturbance footprint for development variables delineated as points or lines.....	852
A-14.	Comparison of Terrestrial Development Index score and greater sage-grouse probability of occurrence	856
A-15.	Relationships between component variables and metrics for the overall Aquatic Development Index and key ecological attributes.....	858
A-16.	Weights by instream distance used for the upstream Aquatic Development Index.....	859
A-17.	Climate variables used in the invasive species models, including values for their percent contribution to the model using climate data from 1971–2000 and 1980–2009.....	864
A-18.	Summary of interpatch distances corresponding to connectivity at local, landscape, and regional levels for baseline conditions and relatively undeveloped areas for terrestrial Conservation Elements evaluated	870
A-19.	Summary of variables used to address landscape-level values and risks for each Conservation Element	872
A-20.	Regression models representing historical fire-climate sensitivities and regression diagnostics..	878
A-21.	Projections of mean area burned for the 2080s.....	880
A-22.	Downscaled climate projection datasets for possible inclusion in climate analysis.....	883

Introduction

This appendix provides additional technical details on the source data and methods used for the Wyoming Basin Rapid Ecoregional Assessment (REA) that are not provided in Chapter 2—Assessment Framework and in the Methods Overview section of the individual chapters for Section II—Change Agents, Section III—Ecological Communities, Section IV—Species, and Section V—Landscape Intactness. For the most part, the description of the methods provided in the chapters is not duplicated in the Appendix. Additional information on the methods is available in the metadata and geographic information system (GIS) programs (Python scripts) used for analyses, which will be served online by the Bureau of Land Management (BLM) at http://www.blm.gov/wo/st/en/prog/more/Landscape_Approach/reas/dataportal.html. Data gaps and uncertainty are also summarized.

Distribution Mapping of Communities and Species

Terrestrial Ecological Community Distribution Maps

To map the distribution of terrestrial ecological communities for the Rapid Ecoregional Assessment (REA), we used LANDFIRE version 1.2.0 Existing Vegetation Types (EVT) (LANDFIRE, 2010). We initially classified each EVT as one of five ecological communities (desert shrublands; grasslands; sagebrush steppe; foothill shrublands and woodlands; and montane/subalpine forests and alpine zone; table A–1). Subsequently, we combined grassland EVT with other community types as described below.

Although LANDFIRE is widely used for mapping vegetation types at broad scales, it can contain classification errors. We used several methods to screen and correct potential classification errors, including using elevation ranges to identify potential misclassifications, review of preliminary community distribution maps by the Assessment Management Team, and cross referencing to other regional vegetation maps (for example, regional Gap Analysis Program [reGAP]). Collectively, these methods eliminated all obvious errors resulting from misclassifications of EVT. However, LANDFIRE is not recommended for use at a 30-m resolution (cell size) because there are mapping inaccuracies at that scale.

We used the literature to establish elevational ranges for EVTs in each ecological community (Beetle and Johnson, 1982; Knight, 1994) and in consultation with experts on vegetation distribution in the Wyoming Basin (Pat Anderson and Dan Manier, Ecologists, U.S. Geological Survey, August 2012, oral commun.; Bob Means, Bureau of Land Management, August 2012, oral commun.). The frequency distribution of elevations for each EVT indicated areas of potential misclassification for isolated cells that fell outside the typical elevational range of each species. Elevation outliers were usually <0.1 percent of the total area for an EVT. To minimize the effects of elevational outliers, all EVTs classified as foothill shrublands and woodlands occurring above 2,900 meters (m) were reclassified as mountain forests and alpine zone community. All EVTs classified as mountain forests occurring below 1,700 m were reclassified as the foothill shrublands and woodlands community.

Table A-1. Cross walk used to classify LANDFIRE Existing Vegetation Types as ecological communities for the Wyoming Basin Rapid Ecoregional Assessment project area.
 [km², square kilometer; NASS, National Agricultural Statistics Service]

Ecological community	LANDFIRE identifier	Existing Vegetation Type	Area (km ²)
Foothill Shrublands and Woodlands	2011	Rocky Mountain Aspen Forest and Woodland	3094.22
Foothill Shrublands and Woodlands	2016	Colorado Plateau Pinyon-Juniper Woodland	1385.20
Foothill Shrublands and Woodlands	2019	Great Basin Pinyon-Juniper Woodland	0.00
Foothill Shrublands and Woodlands	2048	Northwestern Great Plains Highland White Spruce Woodland	4.21
Foothill Shrublands and Woodlands	2049	Rocky Mountain Foothill Limber Pine-Juniper Woodland	1396.32
Foothill Shrublands and Woodlands	2054	Southern Rocky Mountain Ponderosa Pine Woodland	988.72
Foothill Shrublands and Woodlands	2059	Southern Rocky Mountain Pinyon-Juniper Woodland	0.40
Foothill Shrublands and Woodlands	2062	Inter-Mountain Basins Curl-leaf Mountain Mahogany Woodland and Shrubland	1284.59
Foothill Shrublands and Woodlands	2086	Rocky Mountain Lower Montane-Foothill Shrubland	1637.14
Foothill Shrublands and Woodlands	2106	Northern Rocky Mountain Montane-Foothill Deciduous Shrubland	226.06
Foothill Shrublands and Woodlands	2107	Rocky Mountain Gambel Oak-Mixed Montane Shrubland	197.71
Foothill Shrublands and Woodlands	2115	Inter-Mountain Basins Juniper Savanna	76.05
Foothill Shrublands and Woodlands	2117	Southern Rocky Mountain Ponderosa Pine Savanna	121.57
Foothill Shrublands and Woodlands	2119	Southern Rocky Mountain Juniper Woodland and Savanna	0.06
Foothill Shrublands and Woodlands	2123	Columbia Plateau Steppe and Grassland	0.12
Foothill Shrublands and Woodlands	2126	Inter-Mountain Basins Montane Sagebrush Steppe	5400.81
Foothill Shrublands and Woodlands	2179	Northwestern Great Plains-Black Hills Ponderosa Pine Woodland and Savanna	150.49
Foothill Shrublands and Woodlands	2210	<i>Coleogyne ramosissima</i> Shrubland Alliance	0.87
Foothill Shrublands and Woodlands	2211	<i>Grayia spinosa</i> Shrubland Alliance	0.43
Foothill Shrublands and Woodlands	2214	<i>Arctostaphylos patula</i> Shrubland Alliance	0.16
Foothill Shrublands and Woodlands	2217	<i>Quercus gambelii</i> Shrubland Alliance	1090.97
Foothill Shrublands and Woodlands	2220	<i>Artemisia tridentata ssp. vaseyana</i> Shrubland Alliance	14132.80
Desert Shrublands	2001	Inter-Mountain Basins Sparsely Vegetated Systems	1131.54
Desert Shrublands	2007	Western Great Plains Sparsely Vegetated Systems	114.87
Desert Shrublands	2066	Inter-Mountain Basins Mat Saltbush Shrubland	8880.74
Desert Shrublands	2081	Inter-Mountain Basins Mixed Salt Desert Scrub	1258.05
Desert Shrublands	2085	Northwestern Great Plains Shrubland	59.13

Ecological community	LANDFIRE identifier	Existing Vegetation Type	Area (km ²)
Desert Shrublands	2093	Southern Colorado Plateau Sand Shrubland	13.93
Desert Shrublands	2103	Great Basin Semi-Desert Chaparral	6.44
Desert Shrublands	2104	Mogollon Chaparral	0.00
Desert Shrublands	2127	Inter-Mountain Basins Semi-Desert Shrub-Steppe	1143.47
Desert Shrublands	2153	Inter-Mountain Basins Greasewood Flat	1663.47
Montane/subalpine/alpine	12	Snow Ice	
Montane/subalpine/alpine	2006	Rocky Mountain Alpine/Montane Sparsely Vegetated Systems	81.77
Montane/subalpine/alpine	2045	Northern Rocky Mountain Dry-Mesic Montane Mixed Conifer Forest	1.07
Montane/subalpine/alpine	2046	Northern Rocky Mountain Subalpine Woodland and Parkland	3032.23
Montane/subalpine/alpine	2047	Northern Rocky Mountain Mesic Montane Mixed Conifer Forest	45.04
Montane/subalpine/alpine	2050	Rocky Mountain Lodgepole Pine Forest	3423.06
Montane/subalpine/alpine	2051	Southern Rocky Mountain Dry-Mesic Montane Mixed Conifer Forest and Woodland	496.86
Montane/subalpine/alpine	2052	Southern Rocky Mountain Mesic Montane Mixed Conifer Forest and Woodland	241.06
Montane/subalpine/alpine	2055	Rocky Mountain Subalpine Dry-Mesic Spruce-Fir Forest and Woodland	4724.70
Montane/subalpine/alpine	2056	Rocky Mountain Subalpine Mesic-Wet Spruce-Fir Forest and Woodland	299.16
Montane/subalpine/alpine	2057	Rocky Mountain Subalpine-Montane Limber-Bristlecone Pine Woodland	38.44
Montane/subalpine/alpine	2061	Inter-Mountain Basins Aspen-Mixed Conifer Forest and Woodland	1964.30
Montane/subalpine/alpine	2070	Rocky Mountain Alpine Dwarf-Shrubland	537.11
Montane/subalpine/alpine	2140	Northern Rocky Mountain Subalpine-Upper Montane Grassland	824.27
Montane/subalpine/alpine	2143	Rocky Mountain Alpine Fell-Field	0.04
Montane/subalpine/alpine	2144	Rocky Mountain Alpine Turf	1346.32
Montane/subalpine/alpine	2145	Rocky Mountain Subalpine-Montane Mesic Meadow	1684.88
Montane/subalpine/alpine	2166	Middle Rocky Mountain Montane Douglas-Fir Forest and Woodland	1637.57
Montane/subalpine/alpine	2167	Rocky Mountain Poor-Site Lodgepole Pine Forest	124.84
Montane/subalpine/alpine	2169	Northern Rocky Mountain Subalpine Deciduous Shrubland	854.50
Montane/subalpine/alpine	2208	<i>Abies concolor</i> Forest Alliance	17.44
Montane/subalpine/alpine	2227	<i>Pseudotsuga menziesii</i> Forest Alliance	1040.32
Montane/subalpine/alpine	2541	Recently Disturbed Developed Upland Deciduous Forest	0.32
Montane/subalpine/alpine	2542	Recently Disturbed Developed Upland Evergreen Forest	1.31
Montane/subalpine/alpine	2543	Recently Disturbed Developed Upland Mixed Forest	0.12
Riparian	2012	Rocky Mountain Bigtooth Maple Ravine Woodland	83.84

Ecological community	LANDFIRE identifier	Existing Vegetation Type	Area (km ²)
Riparian	2154	Inter-Mountain Basins Montane Riparian Systems	0.73
Riparian	2159	Rocky Mountain Montane Riparian Systems	1050.31
Riparian	2160	Rocky Mountain Subalpine/Upper Montane Riparian Systems	958.15
Riparian	2161	Northern Rocky Mountain Conifer Swamp	57.08
Riparian	2162	Western Great Plains Floodplain Systems	1187.59
Riparian	2180	Introduced Riparian Vegetation	431.76
Riparian	2385	Western Great Plains Wooded Draw and Ravine	8.64
Sagebrush steppe	2064	Colorado Plateau Mixed Low Sagebrush Shrubland	39.63
Sagebrush steppe	2072	Wyoming Basins Dwarf Sagebrush Shrubland and Steppe	2385.03
Sagebrush steppe	2080	Inter-Mountain Basins Big Sagebrush Shrubland	59430.01
Sagebrush steppe	2124	Columbia Plateau Low Sagebrush Steppe	0.81
Sagebrush steppe	2125	Inter-Mountain Basins Big Sagebrush Steppe	16866.12
Multiple communities ¹	31	Barren	
Multiple communities ¹	2135	Inter-Mountain Basins Semi-Desert Grassland	3555.06
Multiple communities ¹	2139	Northern Rocky Mountain Lower Montane-Foothill-Valley Grassland	2191.48
Multiple communities ¹	2141	Northwestern Great Plains Mixedgrass Prairie	3251.85
Multiple communities ¹	2146	Southern Rocky Mountain Montane-Subalpine Grassland	95.20
Multiple communities ¹	2147	Western Great Plains Foothill and Piedmont Grassland	0.79
Multiple communities ¹	2148	Western Great Plains Sand Prairie	322.62
Multiple communities ¹	2149	Western Great Plains Shortgrass Prairie	249.46
Multiple communities ¹	2181	Introduced Upland Vegetation-Annual Grassland	1716.53
Multiple communities ¹	2182	Introduced Upland Vegetation-Perennial Grassland and Forbland	187.90
Multiple communities ¹	2183	Introduced Upland Vegetation-Annual and Biennial Forbland	3148.17
Multiple communities ¹	2195	Recently Burned-Herb and Grass Cover	0.66
Agriculture	63	NASS -Row Crop-Close Grown Crop	287.82
Agriculture	64	NASS-Row Crop	301.76
Agriculture	65	NASS-Close Grown Crop	3439.00
Agriculture	66	NASS-Fallow/Idle Cropland	69.20
Agriculture	75	Herbaceous Semi-Dry ²	281.58
Agriculture	76	Herbaceous Semi-Wet ²	61.25
Agriculture	81	Agriculture-Pasture and Hay	1907.86

Ecological community	LANDFIRE identifier	Existing Vegetation Type	Area (km ²)
Agriculture	82	Agriculture-Cultivated Crops and Irrigated Agriculture	192.96
Agriculture	95	Herbaceous Wetlands ²	1672.07
Agriculture	2198	Recently Burned Herbaceous Wetlands	9.39
Agriculture	2549	Recently Disturbed Pasture and Hayland	1.89
Development	23	Developed-Medium Intensity	44.80
Development	24	Developed-High Intensity	6.10

¹ Elevation ranges and neighborhood analysis was used to classify grassland and barren Existing Vegetation Types into the appropriate ecological community.

² Comparison of Existing Vegetation Types 75, 76, and 95 with aerial imagery indicated these were predominantly agricultural lands. National Wetland Inventory was used to map wetlands for the Wyoming Basin Rapid Ecoregional Assessment aspen functional types.

There were several classification issues for grassland EVT. First, many grassland EVTs spanned multiple communities across a broad elevation range (for example, the EVT “Northern Rocky Mountain Lower Montane-Foothill-Valley Grassland” spanned several community types; table A-1). Second, LANDFIRE classified burned sagebrush shrublands as grasslands in some areas. Finally, most grasslands occurred as small patches throughout all elevations in the Wyoming Basin Ecoregion proper, with the exception of recently burned areas and large areas of prairie grasslands in the eastern buffer of the project area (part of the Northwestern Great Plains ecoregion)(fig. 11-2). As a result of these issues, the Assessment Management Team recommended that grasslands not be addressed as a separate community type for the REA. Rather, they are best considered part of a mosaic with other ecological communities in the Wyoming Basin.

To classify grasslands EVTs into the appropriate community types, grassland cells within the elevational ranges for foothill shrublands and woodlands (2,600–2,900 m) or mountain forests (>2,900 m) were classified into the respective ecological community. For grassland EVTs occurring <2,600 m, we used neighborhood analysis to classify grasslands as desert shrublands or sagebrush steppe, which broadly overlap in elevational range. Grassland EVT cells were classified as the majority community type (desert shrublands or sagebrush steppe) within 210 m of a grassland cell. If neither community achieved a majority within 210 m, grassland cells within 990-m of the majority community were used. Grassland EVTs totaled 1,472 square kilometers (km²), 81 percent of which were reclassified as the sagebrush steppe community. At the request of the Assessment Management Team, we identified the grasslands in the sagebrush steppe distribution map (fig. 11-2), but grasslands were not treated separately in the analyses of the sagebrush steppe community. We used the same proximity analysis to classify the EVT “Barren” into the adjacent dominant ecological community.

The Assessment Management Team identified additional misclassifications of LANDFIRE EVT. Several areas of Russian olive and riparian communities were misclassified as the EVT “Rocky Mountain Aspen Forest and Woodland.” To identify other possible aspen misclassifications, all aspen occurrences below 1,516 m (5,000 feet [ft]) were reclassified using reGAP. In addition, several large areas of known subalpine forest at elevations >2900 m were misclassified as the EVT “Inter-Mountain Basins Curl-leaf Mountain Mahogany Woodland and Shrubland,” which is included in the foothill shrublands and woodlands community. To identify other possible misclassifications of mountain mahogany >2,900 m, we used the reGAP classifications for this EVT; the misclassified areas were predominantly subalpine forests and consequently were included in the mountain forests community type.

Plant Species Distribution Maps

Aspen Forests and Woodlands

We delineated two aspen functional types, foothill and mountain-slope aspen (fig. 15-2). Foothill aspen occurs at lower elevations, typically less than 2,621 m (8,600 ft), within a matrix of sagebrush and other shrubs. Mountain slope aspen occurs across broad elevations from the toe slope to upper subalpine zones, where it intermixes with conifer species (see additional details on aspen functional types in Chapter 10—Aspen). LANDFIRE EVT includes two aspen types “Rocky Mountain Aspen Forest and Woodland” and “Inter-mountain Basin Aspen-mixed Conifer Forest and Woodland,” but these EVTs overlapped broadly in elevation and were not sufficient for use in distinguishing aspen functional types.

To delineate foothill and mountain-slope aspen, we included both aspen EVT types in the following proximity analysis. Because higher elevation aspen typically occurs in proximity to spruce-fir forests, aspen patches (adjacent aspen cells) $\geq 2,220$ m elevation within 240–600 m of spruce-fir LANDFIRE EVT types were classified as mountain-slope aspen. All other aspen patches (adjacent aspen cells) at all elevations and within 0–210 m of the initial mountain-slope aspen patches were also classified as mountain-slope aspen. The remaining aspen cells were classified as foothill aspen. Because the distances used for proximity analysis affected the results, we derived a final estimate of aspen functional types by overlaying the derived maps for all buffer distances (240–600 m; 0–210 m) and used the majority functional type in the combined maps to classify each aspen cell. To eliminate areas that were potentially misclassified as aspen, we only included areas at elevations $> 1,516$ m (5,000 ft) and used the bioclimatic envelope for contemporary aspen (Rehfeldt and others, 2009) and eliminated all aspen cells where the “probability of occurrence” was < 10 percent; these areas were reclassified using reGAP.

Aquatic Ecological Community Distribution Maps

Riparian Areas

The location of riparian areas were identified using vegetation types that included the words riparian, ravine, or floodplain from LANDFIRE EVT (table A–1) and reGAP vegetation. We used 2012 National Agriculture Imagery Program (NAIP) imagery for validation of native and nonnative (Russian olive and tamarisk) riparian areas. There was general correspondence among datasets in the general occurrence of riparian vegetation, particularly when summarizing total area by 6th level watershed. However, the 30-m cells of both LANDFIRE or reGAP lacked close correspondence with the spatial configuration and perimeters of individual riparian patches as compared to NAIP imagery. As a consequence, we were unable to calculate patch metrics or connectivity measures and instead we summarized riparian occurrence at the 6th level watershed. We used LANDFIRE to estimate the locations of riparian in the Wyoming Basin.

Species Distribution Models

Greater Sage-Grouse Habitat Model

We used the general-use sage-grouse habitat model developed by Hanser and others (2011) for the Wyoming Basin to predict potential baseline sage-grouse habitat. Hanser and others (2011) evaluated a variety of sage-grouse habitat models with and without development variables, and the best overall model included several development variables (relating to oil and gas wells, roads, and powerlines). Because distribution maps for baseline conditions in the REA do not explicitly include development variables, we used Hanser and others (2011) top general-use model (low abundance) that included only vegetation and abiotic variables (hereafter “baseline general-use model; provided by Steve Hanser, August 27, 2013, written comm.). The model (a) is shown below (see table A–2 for descriptions of the variables).

$$(a) \text{ Prob} = 1 / (1 + (\exp(-(-5.517441 + 2.891109 \times \text{Big_Sage_1km} + 4.552652 \times \text{Riparian_1km} - 0.0635341 \times \text{Topographic_Roughness_270} + 0.1856618 \times \text{Temp_min} + 0.0022761 \times \text{Elevation}))))$$

Table A-2. Variables used in the sage-grouse baseline general-use model from Hanser and others (2011).
[km, kilometer; m, meter]

Explanatory variable	Variable description
Big_Sage_1km	Proportion of all Wyoming big sagebrush Existing Vegetation Types from LANDFIRE (LANDFIRE identifiers 2125, 2080, 2220, 2126; table A-1) (1-km radius window)
Riparian_1km	Proportion riparian Existing Vegetation Types (LANDFIRE identifiers 2154, 2159, 2160, 2162; table A-1) (1-km radius window)
Topographic_Roughness_270 ¹	Mean topographic roughness index (270-m radius window)
Temp_min	Annual minimum temperature from PRISM ² data 1970–2000
Elevation	Elevation from a 30-m digital elevation model

¹ Topographic roughness index was derived using a script from Riley and others (1999).

² PRISM, Parameter-elevation Relationships on Independent Slopes Model.

Because the spatial extent of the Wyoming Basin used by Hanser and others (2011) was slightly different than the extent of the REA project area, we applied model (a) using the same input data layers (table A-2) to obtain full coverage for the project area. We used a 2,900 m (9,500 ft) elevation threshold to exclude high elevation sites that were unlikely to be used by sage-grouse.

The optimal probability of occurrence threshold used by Hanser and others (2011) to classify the top model output as potential sage-grouse habitat was 0.49. We evaluated the omission errors for a 0.49 threshold using an independent dataset of sage-grouse lek locations; this threshold excluded 18 percent of lek locations (table A-3). Most leks in the southern portion of the Wyoming Basin were included using this threshold, but many leks in the northeastern portion of the Basin were excluded (fig. 23-2). A threshold of 0.25 increased the number of leks included as potential sage-grouse habitat across the entire Basin (table A-3) but led to inclusion of forested and other cover types not typically used by sage-grouse (increased commission error), especially in southern portions of the project area. To minimize these commission errors resulting from the threshold of 0.25, we masked all forested areas and open water in the final baseline model.

Table A-3. Omission error for lek occurrence as a function of probability threshold for the baseline greater sage-grouse general-use habitat model (Hanser and others, 2011).

Probability threshold	Leks omitted (percent)
0.49	18
0.30	7
0.25	5
0.10	1

We also conducted a sensitivity analysis to determine how the choice of probability of occurrence thresholds for baseline habitat affects the assessment of connectivity and patch size for greater sage-grouse. Although a greater amount of potential habitat was predicted by the lower threshold (fig. 23–2), this did not substantially alter the relative effects of development on patch metrics (fig. A–1) or connectivity (fig. A–2). Patch size for relatively undeveloped areas were very similar for both thresholds (fig. A–1). In addition, differences in structural connectivity for relatively undeveloped areas using a threshold of 0.25 compared to 0.49 were small (fig A–2) relative to the differences between baseline and relatively undeveloped areas (tables 23–1 and 23–2). Thus, we conclude that our results are not sensitive to differences in probability of occurrence threshold used to define baseline sage-grouse habitat when evaluated for the entire ecoregion. However, there are local-scale differences (such as northeast or southeast areas of the Wyoming Basin) that may be of interest in application of the results of the REA, and we include all probability values in the baseline habitat map to allow use of other thresholds in future applications.

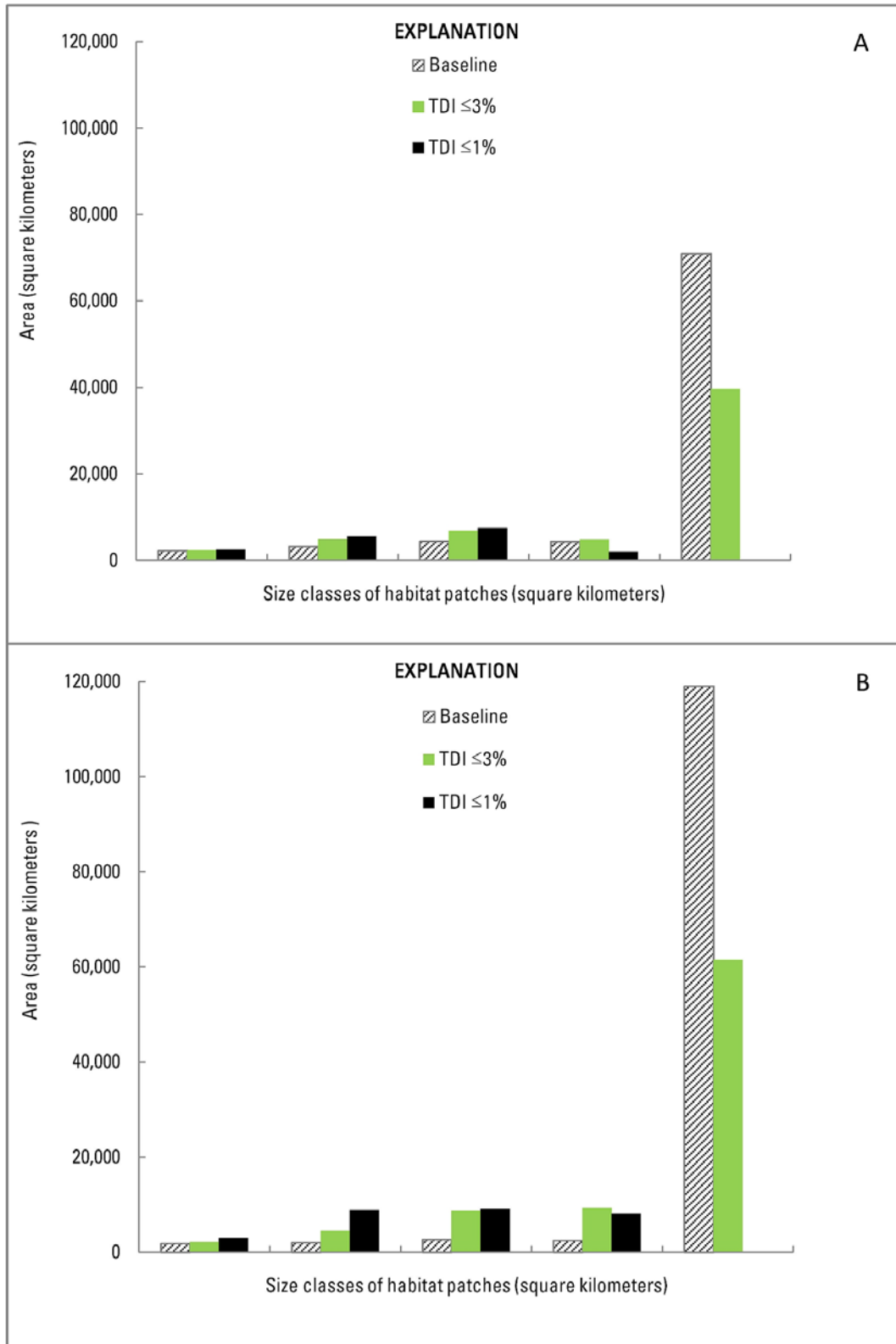


Figure A-1. Patch size of potential greater sage-grouse habitat using a probability threshold of 0.49 (A) and 0.25 (B) for the baseline general-use habitat model.

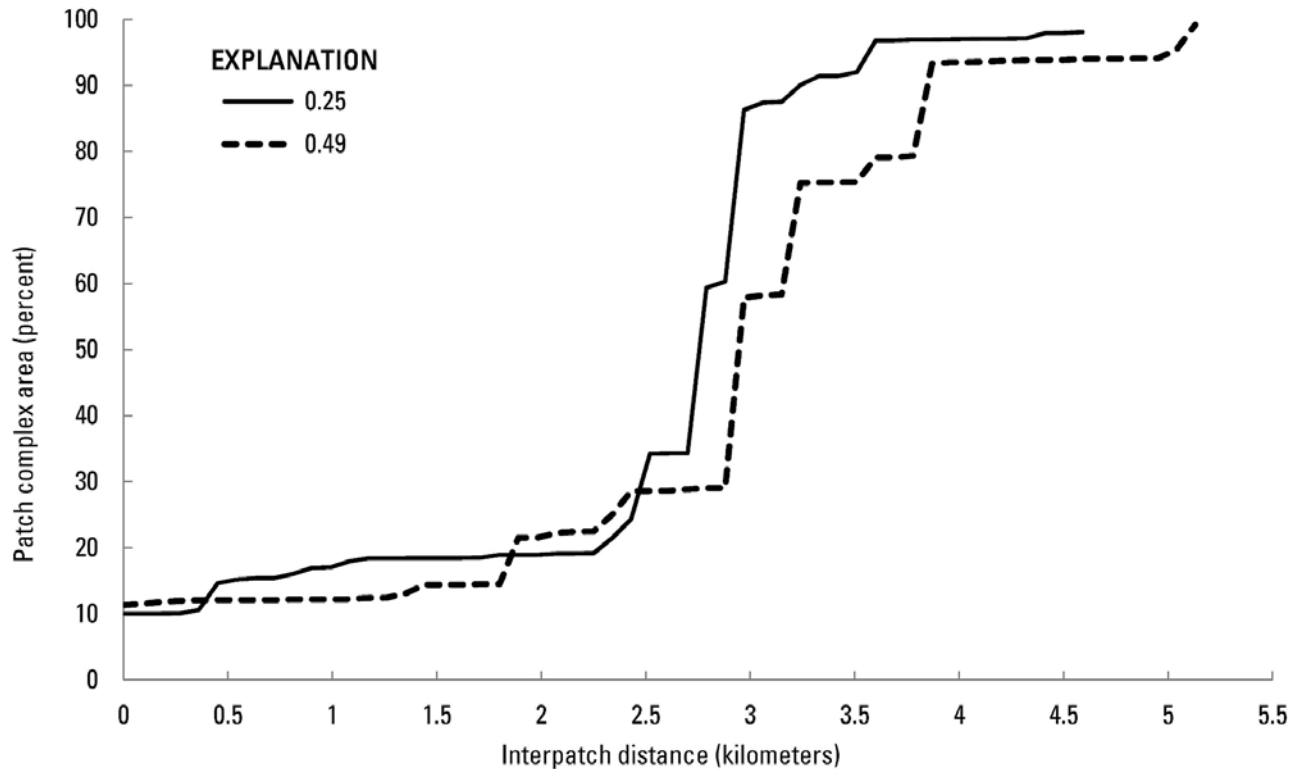


Figure A-2. Structural connectivity of relatively undeveloped greater sage-grouse habitat as a function of interpatch distance at two thresholds in probability of occurrence. Relatively undeveloped areas are defined by a Terrestrial Development Index score ≤ 1 percent. The percent of area represented by the maximum patch size for a given interpatch distance provides an index of structural connectivity.

Species Distribution Modeling using MaxEnt

General Approach

Potential habitat for the spadefoot assemblage, golden eagle, ferruginous hawk, and pygmy rabbit was modeled using a similar approach. For each species, we used MaxEnt (Phillips and others, 2006) to develop a general habitat model that included vegetation and abiotic environmental variables (table A-4). Species occurrence data for the Wyoming Basin ecoregion were provided by the Colorado Natural Heritage Program, Idaho Fish and Wildlife Information System, Montana Natural Heritage Program, Rocky Mountain Bird Observatory, Utah Natural Heritage Program, and Wyoming Natural Diversity Database (table A-5). To minimize discrepancies between occurrences and mapped habitat variables, we excluded occurrences recorded before 1990. Variable importance was assessed by including all variables in an initial model (table A-6). For variables assessed at more than one scale, the scale that explained the largest amount of variance was retained in the final model. When building the distribution model in MaxEnt, we used the default functional relationships (linear, quadratic, multiplicative, threshold, and hinge).

Table A–4. Environmental variables evaluated for contribution to species distribution models for the Wyoming Basin Rapid Ecoregional Assessment.

[km, kilometer; m, meter]

Variable description	Species
Percent cover of all sage species ¹	Brewer's sparrow, ferruginous hawk, pygmy rabbit, sagebrush sparrow, sage thrasher
Average percent cover of all sage species (18 km) ¹	Brewer's sparrow, sagebrush sparrow, sage thrasher
Average percent cover of all sage species (5 km) ¹	Golden eagle
Annual mean temperature ²	Golden eagle, pygmy rabbit
Average temperature of the coldest quarter ²	Pygmy rabbit
Average temperature of the warmest quarter ²	Ferruginous hawk, sage thrasher
Percent cover of barren ground ¹	Brewer's sparrow, ferruginous hawk, sagebrush sparrow, sage thrasher
Percent cover of all big sage species ¹	Brewer's sparrow, pygmy rabbit, sagebrush sparrow, sage thrasher
Average percent cover of big sage species (1 km) ¹	Brewer's sparrow, sagebrush sparrow, sage thrasher
Average percent cover of big sage species (270 m) ¹	Brewer's sparrow, sagebrush sparrow, sage thrasher
Aspect, cosine-transformed ³	Ferruginous hawk, pygmy rabbit
Elevation (30 m) ³	Brewer's sparrow, ferruginous hawk, Golden eagle, sage thrasher, spadeheads
Proportion of agricultural land cover (540 m) ⁴	Ferruginous hawk
Proportion of agricultural land cover (5 km) ⁴	Ferruginous hawk
Proportion of conifer forest land cover (1 km) ⁴	Brewer's sparrow, sagebrush sparrow, sage thrasher
Proportion of conifer forest land cover (270 m) ⁴	Brewer's sparrow, ferruginous hawk, sagebrush sparrow, sage thrasher spadeheads
Proportion of conifer forest land cover (5 km) ⁴	Brewer's sparrow, ferruginous hawk, sagebrush sparrow, sage thrasher
Soil clay content ⁴	Pygmy rabbit
Proportion of grassland land cover (1 km) ⁴	Brewer's sparrow, sagebrush sparrow, sage thrasher
Proportion of grassland land cover (270 m) ⁴	Brewer's sparrow, ferruginous hawk, sagebrush sparrow, sage thrasher
Proportion of grassland land cover (540 m) ⁴	Sagebrush sparrow, sage thrasher
Proportion of grassland land cover (5 km) ⁴	Brewer's sparrow, ferruginous hawk, sagebrush sparrow, sage thrasher
Distance (m) to intermittent water ⁴	Brewer's sparrow, ferruginous hawk, sagebrush sparrow, sage thrasher
Proportion of juniper land cover (270 m) ⁴	Ferruginous hawk
Proportion of juniper land cover (3 km) ⁴	Ferruginous hawk
Proportion of juniper land cover (5 km) ⁴	Ferruginous hawk
Proportion of mixed shrubland land cover (5 km)	Brewer's sparrow, sage thrasher
Normalized Difference Vegetation Index (270 m)	Brewer's sparrow, sagebrush sparrow, sage thrasher
Normalized Difference Vegetation Index (5 km) ⁴	Sagebrush sparrow, sage thrasher
Distance (m) to perennial water	Ferruginous hawk, pygmy rabbit, spadeheads
Proportion of riparian land cover (1 km) ⁴	Golden eagle
Proportion of riparian land cover (540 m)	Brewer's sparrow, sagebrush sparrow, sage thrasher, spadeheads
Soil depth ⁴	Pygmy rabbit
Sagebrush contagion (1 km) ⁴	Pygmy rabbit, sagebrush sparrow
Salt desert shrubland land cover (1 km)	Sagebrush sparrow, sage thrasher

Variable description	Species
Soil sand content ⁴	Pygmy rabbit, spadefoots
Soil silt content ⁴	Pygmy rabbit
Solar radiation index ⁴	Brewer's sparrow, sagebrush sparrow, sage thrasher
Topographic Ruggedness Index (1 km) ⁴	Spadefoots
Topographic Ruggedness Index (270 m) ⁴	Brewer's sparrow, ferruginous hawk, golden eagle, spadefoots
Topographic Ruggedness Index (5 km) ⁴	Brewer's sparrow, ferruginous hawk, sagebrush sparrow, sage thrasher
Percent cover of herbaceous vegetation ¹	Ferruginous hawk, pygmy rabbit
Average percent cover of herbaceous vegetation (510 m) ¹	Pygmy rabbit
Average percent cover of herbaceous vegetation (5 km) ¹	Golden eagle
Euclidean distance to nearest sage grouse lek ⁵	Golden eagle
Precipitation of the wettest quarter ²	Golden eagle, pygmy rabbit
Precipitation of the warmest quarter ²	Sagebrush sparrow, sage thrasher, spadefoots
Average percent cover of all sage species (510 m) ¹	Pygmy rabbit
Percent cover of all shrub species ¹	Brewer's sparrow, ferruginous hawk, pygmy rabbit, sagebrush sparrow, sage thrasher
Average percent cover of all shrub species (990 m) ¹	Pygmy rabbit
Average percent cover of all shrub species (5 km) ¹	Golden eagle
Average height of shrub ¹	Brewer's sparrow, ferruginous hawk, pygmy rabbit, sagebrush sparrow
Slope ³	Ferruginous hawk, golden eagle, pygmy rabbit
Slope (1 km)	Golden eagle, spadefoots
Latitude, Albers U.S. Geological Survey version ⁶	Brewer's sparrow, sagebrush sparrow, sage thrasher
Longitude, Albers U.S. Geological Survey version ⁶	Brewer's sparrow sagebrush sparrow, sage thrasher

¹ Homer and others (2012).

² World Climate (Hijmans and others, 2005).

³ National Elevation Dataset.

⁴ Hanser and others (2012).

⁵ Data provided by the Wyoming Game & Fish Department.

⁶ ArcGIS derived (Esri, 2011).

Table A–5. Data sources and number of occurrences considered for MaxEnt modeling of potential habitat for Conservation Elements in the Wyoming Basin Rapid Ecoregional Assessment.

Data Source	Species			
	Spadefoot assemblage	Golden eagle (nests) ¹	Ferruginous hawk	Pygmy Rabbit
Wyoming Natural Diversity Database	102	470	1477	7851
Colorado Natural Heritage Program	4	121	35	
Montana Natural Heritage Program	33	6		
Rocky Mountain Bird Observatory			1	
Idaho Fish and Wildlife Information System		5	13	
Utah Natural Heritage Program		39	10	
Total	139	641	1536	7851

¹ The Utah Natural Heritage Program provided no dates for the golden eagle occurrences.

Table A–6. Variables, data sources, and percent contribution to the top MaxEnt model for the spadefoot assemblage in the Wyoming Basin Rapid Ecological Assessment.

[m, meter]

Variable description	Contribution (percent)
Elevation	21.1
Proportion of conifer forest land cover (540 m)	19.4
Slope	14.3
Proportion of riparian land cover (540 m)	12.5
Soil sand content	12.2
Distance (m) to intermittent water	8.3
Topographic ruggedness index (270 m)	5.5
Precipitation of the warmest quarter	3.8
Distance (m) to perennial water	2.9

Spadefoot Assemblage

The two spadefoot species were modeled together because there was a good correspondence among habitat features for the two species. The area covered by the model was restricted to the extent of input variables mapped by Homer and others (2012), which was restricted to elevations below 2,377 m (7,800 ft). All occurrences that fell outside this mapped extent were excluded from analysis. We also removed all occurrences that lacked mapping precision (resolution exceeded 3.6 hectares [8.9 acres]) in the data provided by the Colorado Natural Heritage Program and Wyoming Natural Diversity Database. To reduce spatial autocorrelation, we randomly selected one occurrence record from all occurrences separated by <45 m (147.6 ft), leaving 105 records for analysis. After masking out a 45-m buffer around all occurrences, we drew 10,000 background points from the unmasked portion of the analysis area. Initial abiotic and biotic variables considered for input to the MaxEnt model are listed in table A–4 and the variables retained in the top model are listed in table A–6. A 10 percent omission rate was used to identify the probability of occurrence threshold (0.23) for the habitat map.

Golden Eagle

The area covered by the model was restricted to the extent of input variables mapped by Homer and others (2012), which was below 2,377 m (7,800 ft) elevation. All occurrences that fell outside this mapped extent were excluded from analysis. We also removed all occurrences that lacked mapping precision (resolution exceeded 3.6 ha [8.90 acres] resolution) in the data provided by the Colorado Natural Heritage Program and Wyoming Natural Diversity Database. To reduce spatial autocorrelation, we randomly selected one occurrence record from all occurrences separated by <5 kilometers (km) (3.2 miles [mi]) (this corresponds to an average home range size of 100 km² (38.6 square miles [mi²]) Palmer, 1988), leaving 218 records for analysis. We masked a 5-km buffer around all occurrences and drew 10,000 background points from the unmasked portion of the analysis area. Initial abiotic and biotic variables considered for input to the MaxEnt model are listed in table A–4, and the variables retained in the top model are listed in table A–7.

Table A–7. Variables, data sources, and percent contribution to top MaxEnt model for golden eagle nesting habitat in the Wyoming Basin Rapid Ecological Assessment.

[m, meter; km, kilometer]

Variable description	Contribution (percent)
Slope	34.2
Topographic ruggedness index (270 m)	18.1
Percent cover of herbaceous vegetation (5 km)	12.6
Elevation (30 m)	12.1
Annual mean temperature	8.3
Precipitation of the wettest quarter	7.3
Average percent cover of all shrub species	5.4
Average percent cover of all sage species	2

Ferruginous Hawk

The area covered by the model was restricted to the extent of input variables mapped by Homer and others (2012), which was below 2,377 m (7,800 ft) elevation. All occurrences that fell outside this mapped extent were excluded from the analysis. We also removed all occurrences that lacked mapping precision (resolution exceeded 3.6-ha [8.90-ac] resolution) in the data provided by the Colorado Natural Heritage Program and Wyoming Natural Diversity Database. To reduce spatial autocorrelation, we randomly selected one occurrence record from all occurrences separated by <1.4 km (0.9 mi), which corresponds to an average estimate of breeding home-range sizes in Idaho, Utah, and Oregon, (3.4–9.0 km² [1.3–3.5 mi²]) (Smith and Murphy 1973; Janes, 1985), leaving 598 records for analysis. We masked a 1.4-km (0.9-mi) buffer around all occurrences and drew 10,000 background points from the unmasked portion of the analysis area. Initial abiotic and biotic variables considered for input the MaxEnt model are listed in table A–4 and the variables retained in the top model are listed in table A–8.

Table A–8. Variables, data sources, and percent contribution to top MaxEnt model for ferruginous hawk in the Wyoming Basin Rapid Ecological Assessment.

[km, kilometer; m, meter]

Variable description	Contribution (percent)
Topographic ruggedness index (5 km)	32.3
Elevation (30 m)	22.5
Average temperature of the warmest quarter	12.9
Slope	8.5
Proportion of juniper land cover (3 km)	6.0
Proportion of conifer forest land cover (5 km)	5.8
Percent cover of barren ground	3.6
Distance (m) to perennial water	3.4
Proportion of grassland land cover (5 km)	1.6
Average height of shrub	1.1
Percent cover of herbaceous vegetation	0.8
Percent cover of all sage species	0.5
Aspect, cosine-transformed	0.5
Distance (m) to intermittent water	0.3
Percent cover of all shrub species	0.2

Pygmy Rabbit

The area covered by the model was restricted to the extent of input variables mapped by Homer and others (2012), which was below the elevation of 2,377 m (7,800 ft). All occurrences that fell outside this mapped extent were excluded from the analysis. We also removed all occurrences that lacked mapping precision (resolution exceeded 1 ha [2.47 acres]) in the data provided by the Colorado Natural Heritage Program and Wyoming Natural Diversity Database. To reduce spatial autocorrelation, we randomly selected one occurrence record from all occurrences separated by <100 m (328 ft), which corresponds to an average estimate of breeding home-range size in southwestern Wyoming (0.25–1.0 ha [0.62–2.5 acres]) (Katzner and Parker, 1997), leaving 3,066 records for analysis. We masked a 100-m (328.1-ft) radius buffer around all occurrences and drew 10,000 background points from the unmasked portion of the analysis area. Initial abiotic and biotic variables considered for input the MaxEnt model are listed in table A–4 and the variables retained in the top model are listed in table A–9. The probability cutoffs for 5 percent and 10 percent omission error were 0.19 and 0.28 respectively.

Table A–9. Variables, data sources, and percent contribution to top MaxEnt model for pygmy rabbit habitat in the Wyoming Basin Rapid Ecological Assessment.

[m, meter]

Description	Contribution (percent)
Average temperature of the coldest quarter	32.3
Percent cover of all sage species	17.2
Annual mean temperature	14.1
Soil sand content	11.4
Distance (m) to perennial water	6.4
Average height of shrub (990 m)	5.2
Soil clay content	3.3
All sagebrush species contagion	2.4
Precipitation of the wettest quarter	2.4
Slope	1.8
Soil depth	1.2
Soil silt content	1.2
Average percent cover of all sage species (510 m)	0.9
Average percent cover of herbaceous vegetation (510 m)	0.3

Species Occupancy Modeling for Sagebrush-Obligate Songbirds

Rocky Mountain Bird Observatory provided 2008–2013 survey data for all three sagebrush-obligate songbirds (Rocky Mountain Bird Observatory, 2013). To maintain sample independence, we only retained detections of adults that were ≤ 125 m (410.1 ft) from the observer. Additionally, we randomly selected one occurrence wherever occurrences were < 125 m apart and removed detections categorized as migrants, flyovers, and incidentals. The 6-minute point counts were divided into three, 2-minute time periods for occupancy analyses. An encounter was defined as ≥ 1 detections during a 2-minute time period. Surveys without any detection of the species of interest were used as absences in the encounter history. Initial variables tested are listed in table A–4. Thresholds for identifying suitable sagebrush-obligate habitat minimized omission and commission errors and were verified with independent datasets from the Idaho Fish and Wildlife Information System, Montana Natural Heritage Program, Utah Natural Heritage Program, and Wyoming Natural Diversity Database.

Brewer’s Sparrow

The variables and associated parameters for variables in the top occupancy model for Brewer’s sparrow are provided in table A–10. The model was developed using 3,621 unique encounter histories. The binary surface used a 5 percent omission error of the training; that is, Rocky Mountain Bird Observatory data resulted in 6.5 percent omission error in the 1,615 independent test-data locations (includes data from Idaho Fish and Game, Montana Natural Heritage Program, Utah Natural Heritage Program, and Wyoming Natural Diversity Database).

Table A-10. Variables and logit link function parameters for the Brewer's sparrow occupancy model.
[s.e., standard error; m, meter; km, kilometer]

Variable	Beta	s.e.	95 percent confidence interval	
			Lower	Upper
Intercept	-115.635	0.000	-115.635	-115.635
Normalized difference vegetation index (270 m) ¹	-18.711	7.204	-32.831	-4.591
Normalized difference vegetation index (270 m)	16.282	6.878	2.802	29.763
Proportion of mixed shrubland land cover (5 km)	15.737	13.985	-11.674	43.148
Proportion of conifer forest land cover (1 km)	7.998	2.203	3.680	12.315
Proportion of riparian land cover (540 m)	-3.881	1.266	-6.363	-1.400
Proportion of grassland land cover (270 m)	-0.898	0.713	-2.295	0.499
Average percent cover of big sage species (270 m)	0.759	0.162	0.442	1.076
Average percent cover of big sage species (270 m) ¹	-0.041	0.009	-0.059	-0.024
Percent cover of all sage species	0.456	0.102	0.256	0.656
Percent cover of all sage species ¹	-0.011	0.004	-0.018	-0.004
Solar radiation index	0.319	0.050	0.221	0.416
Solar radiation index ¹	-0.001	0.000	-0.001	-0.001
Topographic ruggedness index (5 km)	-0.114	0.015	-0.144	-0.083
Percent cover of barren ground	0.030	0.012	0.007	0.053
Elevation (30 m)	-0.023	0.005	-0.033	-0.012
Elevation (30 m) ¹	0.000	0.000	0.000	0.000
Average height of shrub	0.005	0.019	-0.033	0.042
Distance (m) to intermittent water	-0.001	0.000	-0.001	0.000

¹Squared term.

Sagebrush Sparrow

The variables and associated parameters in the top occupancy model for sagebrush sparrow are provided in table A–11. The model was developed using 4,568 unique encounter histories. The binary surface used a 5 percent omission error of the training; that is, Rocky Mountain Bird Observatory data resulted in 5.3 percent omission error in the 761 independent test data locations (includes data from Wyoming Natural Diversity Database).

Table A–11. Variables and logit link function parameters for the sagebrush sparrow occupancy model. [s.e., standard error; km, kilometer; m, meter]

Variable	Beta	s.e.	95 percent confidence interval	
			Lower	Upper
Intercept	-126.829	0.000	-126.829	-126.829
Normalized difference vegetation index (5 km)	-9.388	1.102	-11.548	-7.228
Proportion of conifer forest land cover (5 km)	7.627	1.258	5.161	10.093
Salt desert shrubland land cover (1 km)	-0.779	0.694	-2.139	0.582
Percent cover of all sage species	0.557	0.108	0.345	0.768
[Percent cover of all sage species] ¹	-0.003	0.007	-0.017	0.011
Percent cover of all big sage species	-0.116	0.099	-0.310	0.078
[Percent cover of all big sage species] ¹	-0.012	0.007	-0.026	0.003
Topographic ruggedness index (5 km)	-0.073	0.010	-0.092	-0.054
Solar radiation index	0.018	0.005	0.009	0.028
Sagebrush contagion	0.009	0.004	0.002	0.016
Distance (m) to intermittent water	0.000	0.000	-0.001	0.000

¹Squared term.

Sage Thrasher

The variables and associated parameters for variables in the top occupancy model for sage thrasher are provided in table A–12. The model was developed using 4,012 unique encounter histories. The binary surface used a 5 percent omission error of the training; that is, Rocky Mountain Bird Observatory data resulted in 8.6 percent omission error of the 964 independent testing data locations (includes data from Idaho Fish and Game, Montana Natural Heritage Program, and Wyoming Natural Diversity Database).

Table A-12. Variables and logit link function parameters for the sage thrasher occupancy model.
[s.e., standard error; km, kilometer]

Variable	Beta	s.e.	95 percent confidence interval	
			Lower	Upper
Intercept	-3.870	0.000	-3.870	-3.870
Proportion of mixed shrubland land cover (5 km)	71.045	13.611	44.366	97.723
Normalized difference vegetation index (5 km)	-5.728	0.345	-6.405	-5.051
Proportion of conifer forest land cover (1 km)	1.603	1.010	-0.376	3.582
Proportion of grassland land cover (1 km)	1.597	0.000	1.597	1.597
Salt desert shrubland land cover (1 km)	1.483	1.075	-0.623	3.590
Percent cover of all sage species	0.635	0.090	0.459	0.810
[Percent cover of all sage species] ¹	-0.014	0.002	-0.019	-0.010
Percent cover of all big sage species	-0.166	0.069	-0.301	-0.031
Average temperature of the warmest quarter	-0.089	0.000	-0.089	-0.089
Topographic ruggedness index (5 km)	-0.052	0.000	-0.052	-0.052
Precipitation of the warmest quarter	-0.039	0.000	-0.039	-0.039

¹Squared term.

Change Agents

Development

Terrestrial Development Index

The Terrestrial Development Index (TDI) quantifies levels of development intensity, including agriculture, roads and railroads, energy and minerals, transmission lines, and urban development. The primary variables associated with terrestrial development (table 2–6) were compiled; to facilitate compilation of the development variables, we used a common metric—surface disturbance—to quantify each variable. The TDI is derived from the percent of surface disturbance footprint for all terrestrial development variables in a 16-km² (6.18-mi²) moving window. An overview of methods for the TDI is described in Chapter 2—Assessment Framework.

To map the surface disturbance footprint from roads and railroads, we created buffers using the estimated surface disturbance footprint from various road types and railroads (table A-13). An initial examination of the TDI scores indicated large discrepancies at state boundaries resulting from differences in data sources, primarily because of the comprehensive road data available for Wyoming (O’Donnell and others, 2014) compared to Topographically Integrated Geographic Encoding and Referencing (TIGER) data used for the other states. Spot checking of NAIP imagery and TIGER indicated most of the omissions were in the vicinity of energy fields. We enhanced the TIGER data for Colorado, Utah, Idaho, and Montana by identifying energy fields and digitizing roads not captured by the TIGER data. Four-wheel drive roads were not digitized in the enhanced TIGER data.

Table A-13. Surface disturbance buffers used for quantifying the surface disturbance footprint for development variables delineated as points or lines. Buffers extend on both sides of lines and as a radius for points. [m, meter; ha, hectare]

Development variable	Attribute type	Mean size of buffer
Interstates ¹	Line	45 m
Highways ¹	Line	15 m
Secondary roads ¹	Line	10 m
Four-wheel drive roads ¹	Line	4 m
Railroads ²	Line	10 m
Transmission lines ³	Line	10 m
Well pad ⁴	Point	56-m radius (1 ha)
Wind turbine pad ³	Point	72-m radius (1.6 ha) ⁶
Silica mine ⁵	Point	22-m radius (6.5 ha)
Uranium mine ⁵	Point	60-m radius (115 ha)
Stone mine ⁵	Point	74-m radius (173 ha)

¹ O'Donnell and others (2014); Topological Integrated Geographic Encoding and Referencing (TIGER) from U.S. Census data.

² Federal Railroad Administration (FRA) data.

³ Federal Aviation Administration (FAA) data; Sagebrush and Grassland Ecosystem Map (SAGEMAP; at <http://sagemap.wr.usgs.gov/>).

⁴ State Oil and Gas Commissions.

⁵ U.S. Geological Survey (2012).

⁶ Denholm and others (2009).

The surface disturbance footprint for energy and minerals was mapped by creating buffers for oil and gas wells, wind turbines, and mine point locations (table A-13). Oil and gas wells within a 30-m (98.42-ft) radius buffer were combined as a single pad. The mean surface area footprint for mines was estimated by digitizing a random sample of each mine type for the project area. The surface area footprint for linear energy transmission structures was created using a 10-m (32.81-ft) buffer to all transmission lines. After comparing multiple state and regional data sources, we used LANDFIRE agriculture EVT_s to map the surface area of agriculture for the Wyoming Basin, because it was consistent across state boundaries and provided the most comprehensive regional dataset for agricultural lands. The surface disturbance footprint for urban development was mapped by combining areas designated as medium-intensity (EVT 23) and high-intensity (EVT 24) development for LANDFIRE and National Agricultural Statistics Service (NASS; classes 123 and 124) data (table A-1). To calculate the overall development index, the surface disturbance footprints for all development variables were compiled into an overall surface disturbance footprint raster by taking the maximum disturbance value in each cell. The compiled footprint map was used in a moving window analysis to calculate the percent development within a 2.25-radius (16-km²) moving window analysis.

Selection of Moving-Window Size

We conducted preliminary analyses to determine the most appropriate window size for quantifying the total surface disturbance for the TDI. Sample units that are too small can result in very little surface disturbance per sampling unit such that the score essentially reflects the presence or

absence of surface disturbance, but such scales provide little information about development intensity. Sample units that are too large may average a wide range of development intensities, resulting in low variation among samples. To determine an optimal window size, we conducted an analysis of variability in total surface disturbance across a range of square window sizes (0.8–441 km² [0.3–170.3 mi²]; fig. A–3). For each window size, we generated 10,000 randomly selected (with replacement) windows within the project area and calculated the total, mean, and standard deviation of surface disturbance in each window. A 3-segment regression model fit to the trend in the coefficient of variation by window size revealed an inflection point for window sizes of 9–16 km² (3.5–6.2 mi²) (fig. A–3), indicating a reasonable scale for smoothing finer-scale variation while retaining a representative level of variability at broad scales. Because the REAs for other ecoregions had used a 16-km² (6.2-mi²) grid for analysis units, we selected the upper range of this inflection point to provide consistency in the scale of analysis or reporting units among REAs. We also evaluated how moving window size can affect the TDI map by generating multiple TDI maps using 4-, 16-, and 130-km² (1.5-, 6.2-, and 50.2-mi², respectively) moving window sizes (fig. A–4).

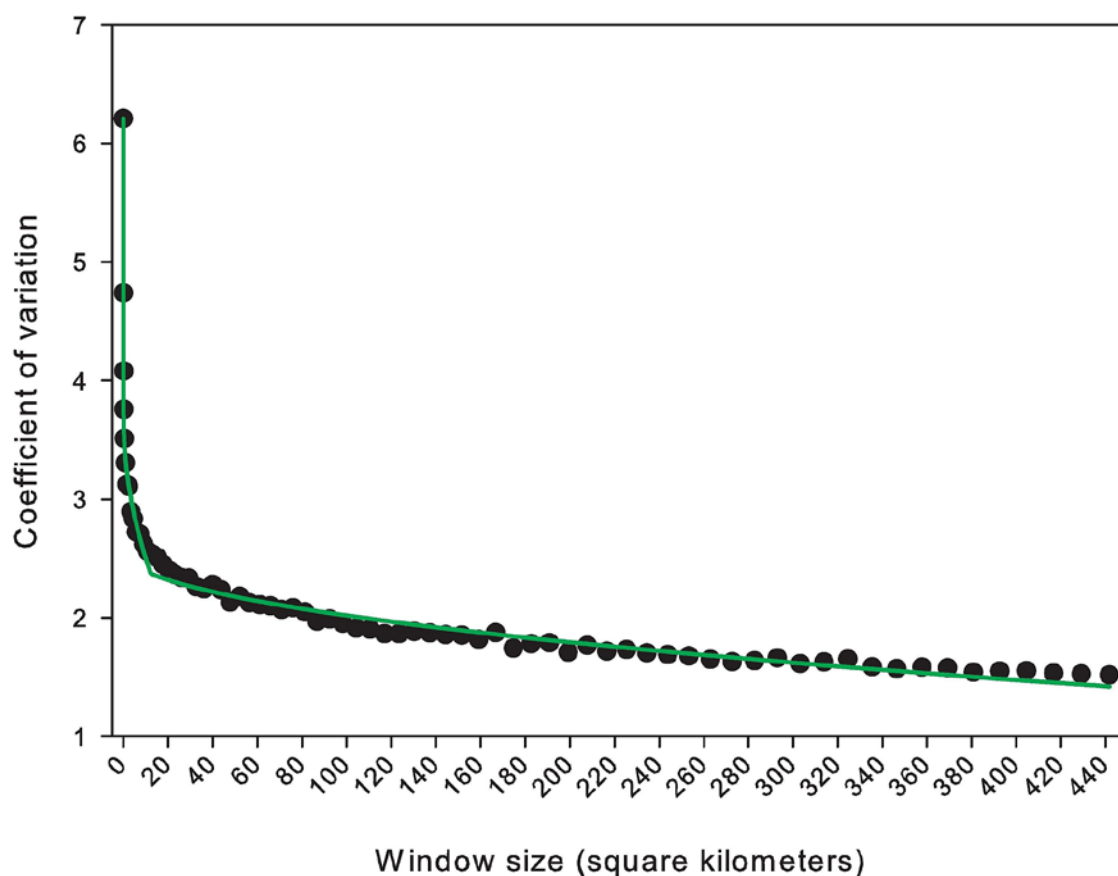


Figure A–3. Evaluation of optimal window size for calculating the Terrestrial Development Index for the Wyoming Basin project area. Window size reflects the length of one side of a sampling unit. The green line represents a 3-segment regression ($R^2 = 0.9873$). The inflection point of the regression line at 9–16 km² (3.5–6.2 mi²) represents an optimal window size.

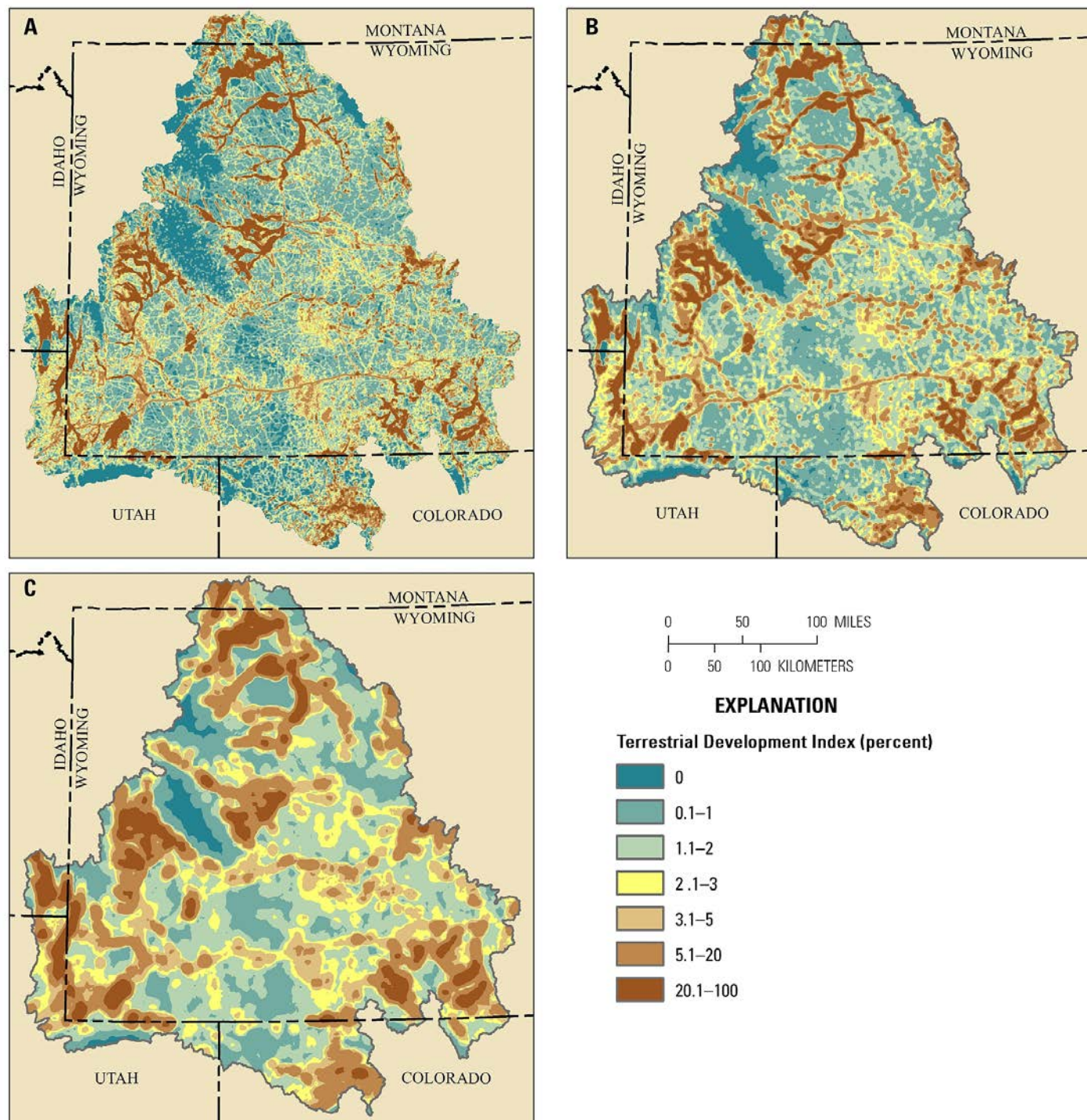


Figure A-4. Terrestrial Development Index scores for several sizes of moving windows: (A) 4 square kilometers (km²) (1.6 square miles [mi²]), (B) 16 km² (6.2 mi²), and (C) 130 km² (50.2 mi²). Only the 16 km² window size was used for the Wyoming Basin Rapid Ecoregional Assessment because it was at the optimal threshold for analysis scale (see fig. A-3).

Selection of Terrestrial Development Index Breakpoints

We used 10 equal subsets (quantiles) to identify potential breakpoints for the TDI scores at 16 km². The upper values of the breakpoints were 0, 0.39, 0.78, 1.17, 2.0, 3.1, 5.1, 9.8, 23.9 and 100. To provide meaningful and intuitive breaks for visualization purposes, we used integer values roughly corresponding the 10 quantiles, using the following upper values, 0, 1, 2, 3, 5, 20, and 100). Some of the higher classes were combined to limit the number of classes to seven, as recommended by the Assessment Management Team. The continuous TDI scores were retained for analysis purposes.

Comparison of the Terrestrial Development Index to Other Similar Approaches

Human modification of landscapes includes the conversion or alteration of vegetation resulting from human activities including development (such as roads, energy and mineral extraction, agriculture, livestock grazing, and urban development), associated disturbance from human activities, introduction of invasive nonnative species, timber management, and fire suppression. The degree of vegetation alteration varies among the types of development, such as an interstate highway compared to an agricultural field. However, quantifying the variety of direct and indirect effects of human modification of the landscape is challenging at the ecoregion level because the response to development varies among species and has not been studied for most species. The direct conversion of natural vegetation by development (or “footprint”) is the most widely available information at the ecoregion level and provides a direct measure of development that can be applied to both communities and species, as well as at the ecoregion level. Although there are methods that address both the footprint and the intensity of human activities associated with development that can negatively affect species (such as Theobald, 2013), these methods require additional assumptions about intensity levels, which are not likely to be applicable to all species. In addition, the intensity of activity is often proportional to the size of the footprint, and may be sufficiently represented by the footprint area without including weighting factors. For example, an interstate highway is much wider and typically has greater traffic volumes than a secondary road.

In contrast to removal or conversion of vegetation types by some development activities, agricultural areas may still retain some native vegetation (such as pastures) or may be used by species for some portion of their life cycle. Some have used weights to address this issues (Theobald, 2013). We conducted a sensitivity analysis to determine how weighting the intensity of impact for row crops (0.5) and pastures (0.25) affected the TDI score. Because of the spatial patterning of agricultural lands, which often cover multiple adjacent cells (900 square meters [m²]) within the 16-km² moving window, the TDI scores for agricultural lands typically exceeded 5 percent; consequently, agricultural areas would still have high development levels and the use of weightings complicates the interpretation of the TDI score, which without weights simply reflects the footprint area. In addition, the focus of the REAs is on intact areas, and the composition of agricultural lands differs from native vegetation. For these reasons, we did not include weights in the TDI.

Because of the challenges with unambiguously quantifying intensity, we focused on the landscape-level effects of the development footprint to evaluate landscape intactness and identify the relatively undeveloped areas. The TDI is similar to the west-wide “human footprint” model of Leu and others (2008), but differs in several respects. First, we focused the TDI on the surface disturbance footprint and did not include other components used in the human footprint model including, invasive plant risk, presence of corvids, dogs, and cats, or fire ignitions. Second, we used different source data for many of the input variables because of the availability of regional datasets and in some cases more recent data, and used slightly different buffer distances to create the footprint for point and line data

layers (table A–13). The human footprint model used contagion to evaluate the fragmenting effects of development, whereas we used patch size and structural connectivity. Finally, we used a smaller analysis unit (15 m) for quantifying the surface disturbance footprint (compared to 180 m [590.56 ft]), and a smaller moving window size (16 km² [6.2 mi²]) for calculating the TDI (compared to 2,975 km² [1,148.6 mi²]) used in the human footprint model because the smaller analysis units provided more detail for the smaller spatial extent of the Wyoming Basin compared to the human footprint model (see Selection of Moving Window Sizes section above for additional details on the scale of analysis units).

Validation of Terrestrial Development Index

To evaluate the validity of the TDI for representing species-level threats posed by development, we compared the TDI score with the predicted probability of greater sage-grouse occurrence (using the top general-use habitat model, which included development variables (Hanser and others, 2011). We randomly selected 150,000 cells (approximately 1 percent of the project area) and compared the mean probability of occurrence for each TDI class (table A–14). Using a probability threshold of 0.49 (Hanser and others, 2011), the results indicated that a TDI score of 2–3 percent may represent a potential threshold in development levels for greater sage-grouse occurrence (table A–14; fig. A–5). For TDI >3 percent, the mean probability of occurrence drops dramatically and remains low for TDI >5 percent (table A–14). Although there is considerable variation in the predicted probability of occurrence and TDI scores (fig A–5), the central tendency of this relationship supports the use of TDI as an index of potential threats of development in the Wyoming Basin REA.

Table A–14. Comparison of Terrestrial Development Index score and greater sage-grouse probability of occurrence. The probability of occurrence is derived from the top general-use habitat model, which includes development variables from Hanser and others (2011).

[>, greater than]

Terrestrial Development Index score (percent)	Mean probability of occurrence ¹	Sample size ²
0	0.45	270
0.1–1	0.53	33,193
1–2	0.53	46,359
2–3	0.50	21,706
3–5	0.47	16,823
5–10	0.42	14,182
10–20	0.41	8,886
>20	0.39	8,684

¹ The optimal threshold for greater sage-grouse probability of occurrence for this model was 0.49, which generally corresponds to a Terrestrial Development Index score of 2–3 percent.

² A random sample was generated for comparing the Terrestrial Development Index score and the probability of occurrence. Very little greater sage-grouse habitat had a Terrestrial Development Index score of 0 percent because this score usually occurs at elevations that are higher than where sage-grouse typically occur.

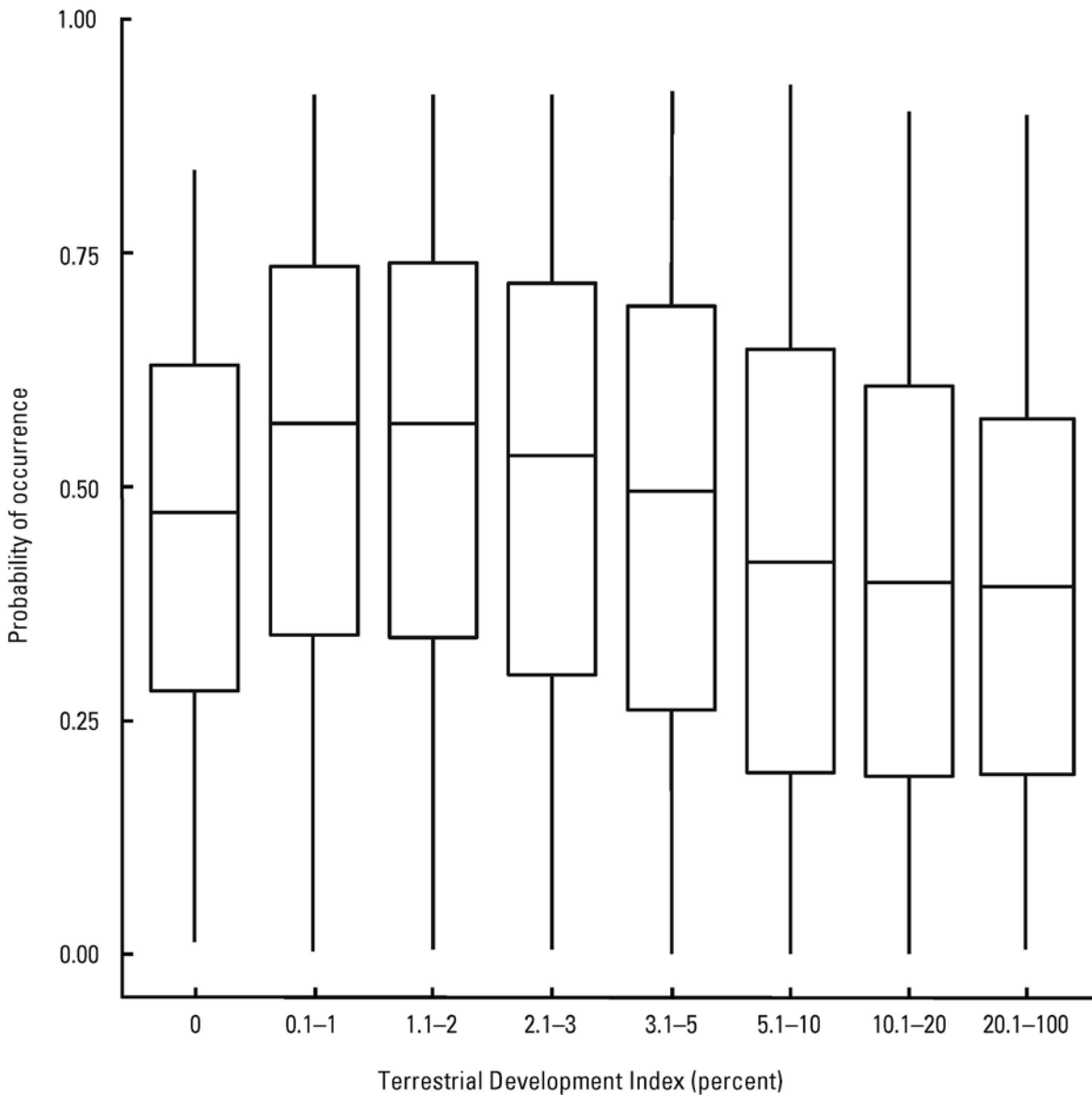


Figure A-5. The relationship between the predicted probability of occurrence for greater sage-grouse and the Terrestrial Development Index (TDI). The probability of occurrence is derived from the top general-use habitat model, which includes development variables, from Hanser and others (2011). Median TDI scores are represented by the horizontal line dividing the box, 25 percentile (lower line of the box), 75 percentile (upper line of the box), and minimum (maximum) scores by the lower (upper) extent of the vertical lines for each box.

Aquatic Development Index

Watershed land use has repeatedly been shown to be a good predictor of stream and riparian degradation (Paukert and others, 2011). Table A–15 summarizes the variables and metrics serving as indicators for key ecological attributes associated with streams and rivers. Variables and metrics can address more than one ecological attribute. For example, surface disturbance directly impacts the habitat quality of riparian zones, but the presence of impervious surfaces also can alter flow regimes. Likewise, structures that alter connectivity (roads, dams, and water diversions) can alter flow or sedimentation regimes. We used the Terrestrial Development Index to address multiple ecological attributes (table A–15), such as increased sedimentation in areas of higher agriculture use. Water diversions can be used as an indicator of altered flow regime on relatively small streams, whereas dams can be used as an indicator of altered flow regime on relatively large streams and rivers.

Table A–15. Relationships between component variables and metrics for the overall Aquatic Development Index and key ecological attributes.

[km², square kilometers]

Variable	Metric	Key ecological attribute				
		Flow regime	Sedimentation regime	Riparian zone	Connectivity	Water quality
Surface disturbance	Variables in the Terrestrial Development Index (km ²) per catchment area (km ²)	X	X	X		X
Road crossings	Number of road crossings per catchment area (km ²)		X		X	
Water use	Number of dams	X			X	
	Number of water diversions per catchment area (km ²)	X			X	
Water quality	303d waterways km per catchment area (km ²)					X

We developed an Aquatic Development Index (ADI) based on the synoptic human threat index developed by Annis and others (2010). This approach quantifies development at two hydrologically defined scales (local catchment for a given stream segment and upstream contributing area). In addition, instream distance measures are used to weight the potential effects of development for the upstream portion of the synoptic human threat index (table A–16, figs. A–6 and A–7). Unique subset combinations for variables included in the full ADI can be derived (fig. 4–6) such as transportation or energy and minerals.

Table A-16. Weights by instream distance used for the upstream Aquatic Development Index.
[km, kilometer]

Weight (multiplier)	
15	0-2
7	2.1-10
3	10.1-100
1	>100

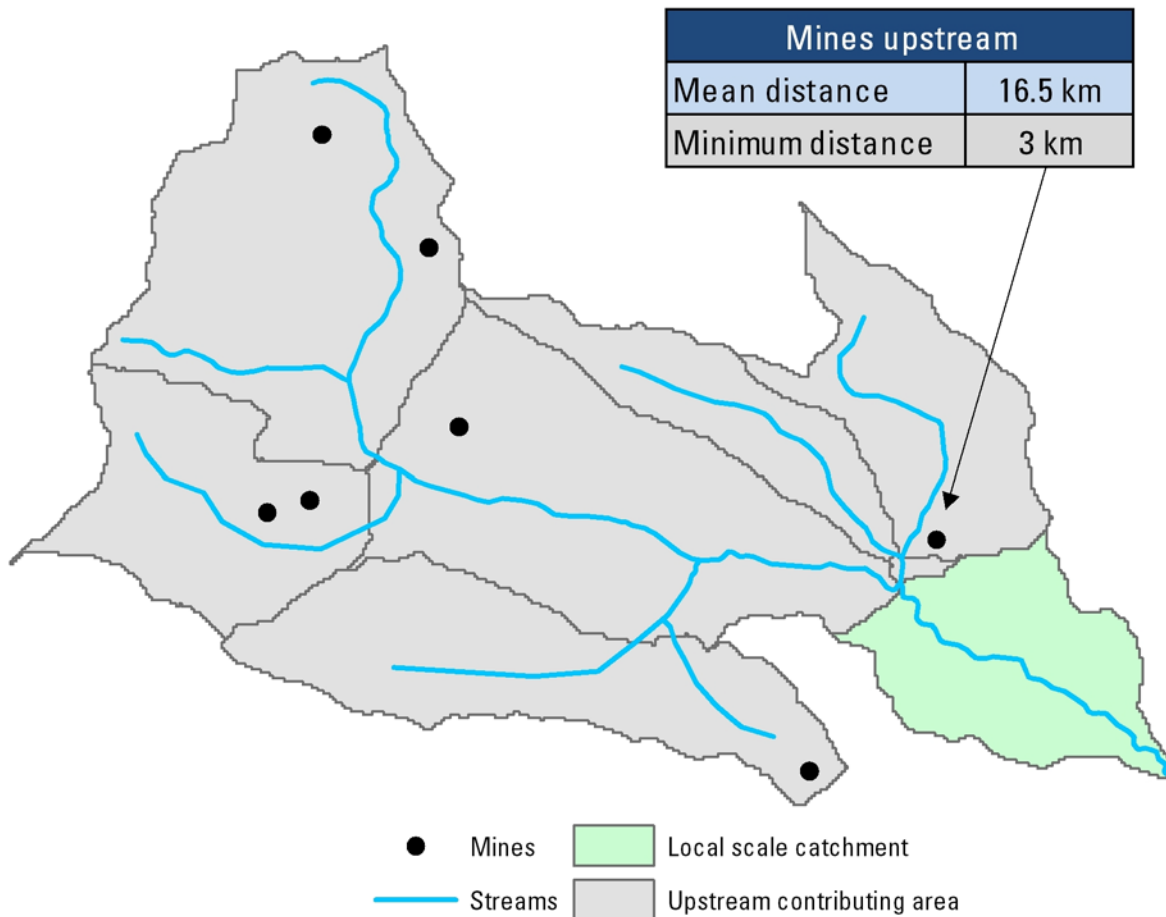
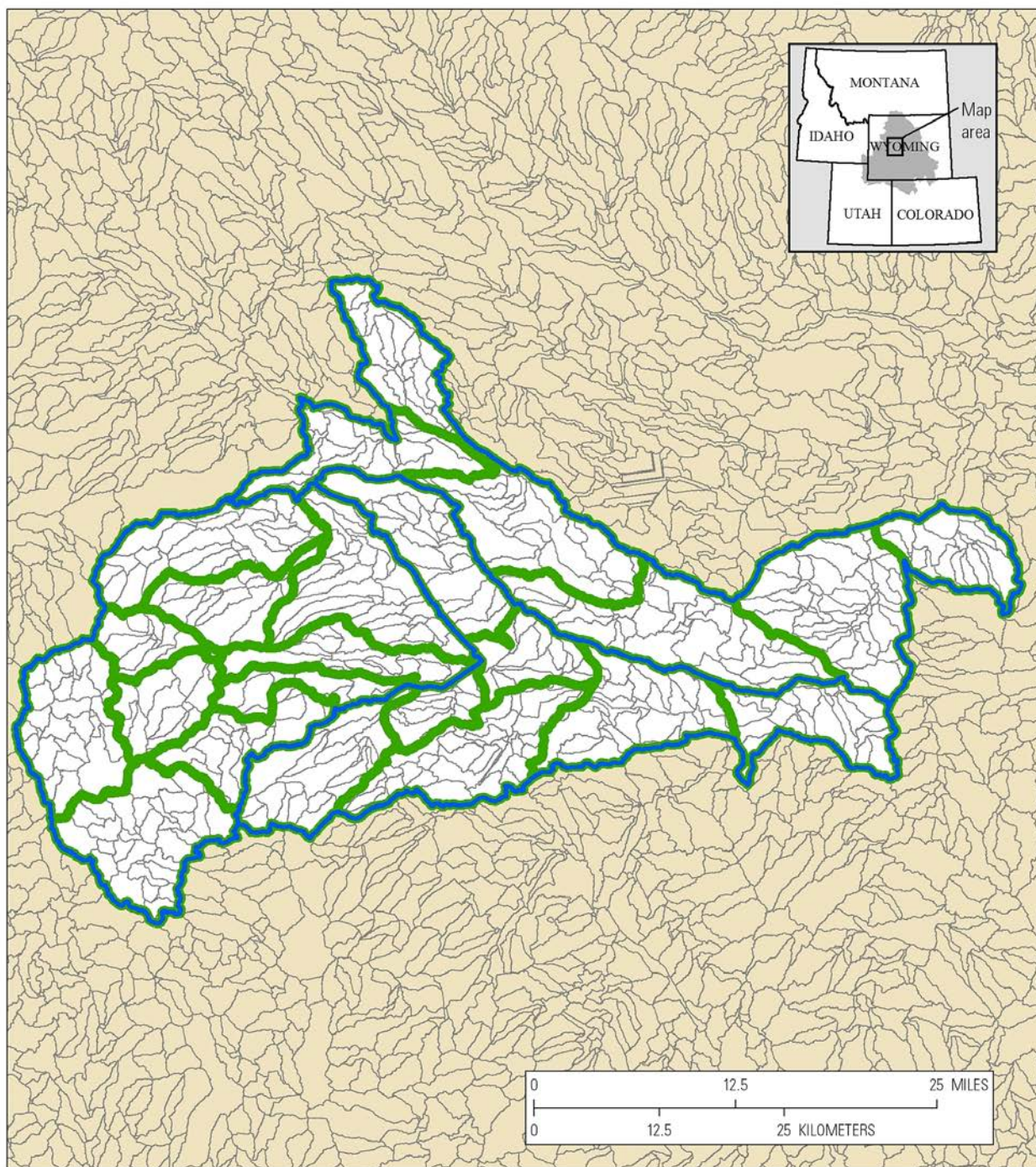


Figure A-6. Diagram of the local and upstream contributing area used for calculating the overall Aquatic Development Index. Examples of distance weights for the upstream contributing area are shown in the inset box. [km, kilometers]



EXPLANATION

- Fifth-level watersheds
- Sixth-level watersheds
- Catchments

Figure A-7. Examples of nested catchments and watersheds in the Wyoming Basin Rapid Ecoregional Assessment project area.

Perennial streams were defined from National Hydrography Dataset (NHD) (2012) flow line data. Stream segments and associated catchments were defined at a catchment threshold size of 3 km² using the flow accumulation output and the ArcHydro Stream Definition tool (Esri Water Resources Team, 2011). Additional processing was required for catchments in the Great Divide Basin (a closed basin). The upstream contributing area was calculated from each pour point, which is the location furthest downstream in each catchment. All dams and water bodies (lake/pond, reservoirs) spatially coincident with a dam location were identified, converted from polygonal to raster, given a value of 100, and subtracted from the reconditioned and filled digital elevation model used to define the local catchments. This captures the loss of hydrological connectivity and flow resulting from dams. A flow direction raster was derived, which was used in conjunction with the ArcGIS watershed tools to create the upstream watersheds to include the influence of dams from the pour points per catchment. We assumed that water bodies overlapping dams are reservoirs and represent impediments to upstream and downstream flows.

For each catchment, we calculated local and upstream ADI (fig. A–6). The local ADI is derived using the local-scale catchment, whereas upstream ADI is derived from upstream contributing area. The values for each variable were ranked and rescaled from 0 to 100 using the SciPy rank data function within the stats module (SciPy, 2013). The values for all the ranked variables are summed by catchment (local or upstream) and normalized from 0 to 100. The overall ADI by catchment is derived by summing the local and upstream ADI values and normalizing from zero to 100 across (fig. A–8).

We used Wyoming Stream Integrity Index (WSII) (Hargett and ZumBerge, 2006; Hargett, 2011) to evaluate the correlation between the ADI and the integrity of streams. The WSII uses macroinvertebrate community-level metrics that reflect the degree to which biological communities differ from that expected for reference conditions. Despite limitations in the WSII, there was good correspondence between the mean WSII and the upstream ADI (fig. A–9) supporting the use of the ADI as an index of risk to watersheds. ADI scores <20 corresponded to median WSII scores of 70 indicating high stream integrity, whereas ADI scores ≥40 corresponded to median WSII scores <30 indicating low integrity for the stream macroinvertebrate communities (Hargett and ZumBerge, 2006).

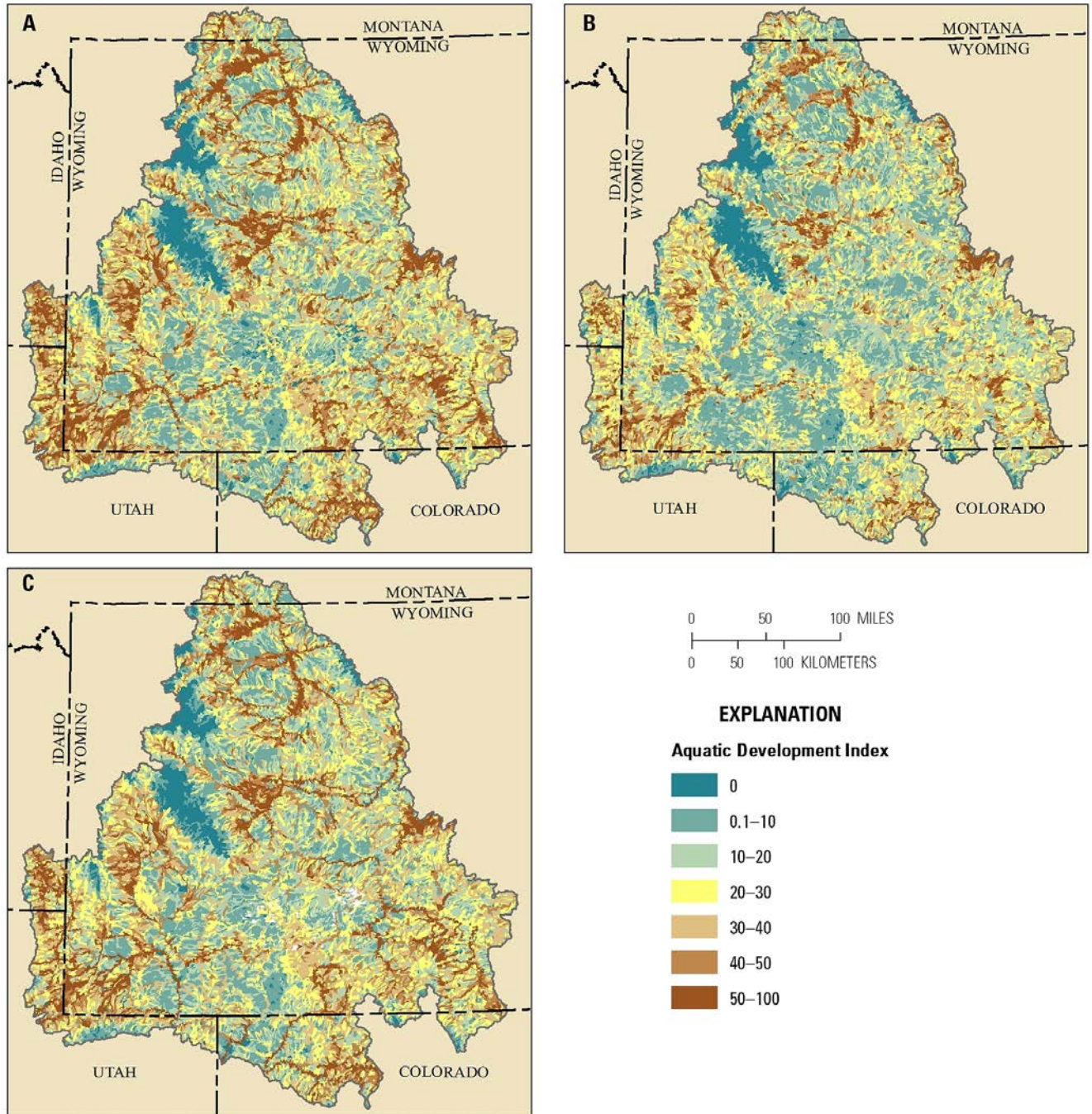


Figure A-8. Aquatic Development Index (ADI) for the Wyoming Basin Rapid Ecoregional Assessment project area. (A) ADI, (B) local ADI, and (C) upstream ADI.

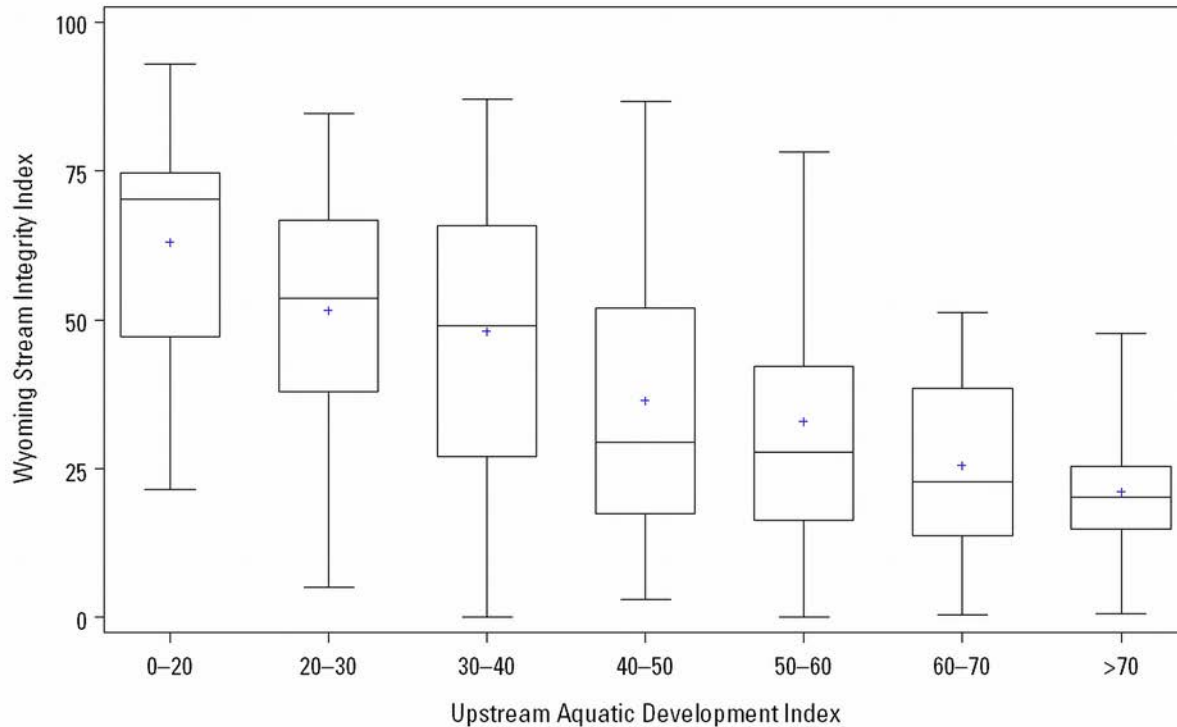


Figure A-9. Correspondence between the Wyoming Stream Integrity Index and upstream Aquatic Development Index (ADI) scores for the Wyoming Basin Rapid Ecoregional Assessment. Mean upstream ADI score is represented by the plus sign, median score by the horizontal line dividing the box, 25 percentile (lower line of the box), 75 percentile (upper line of the box), and minimum (maximum) scores by the lower (upper) extent of the vertical lines for each box. Upstream ADI shows the closest correspondence to the Wyoming Stream Integrity Index compared to ADI or Local ADI. Relatively undeveloped areas have an ADI score <20.

Invasive Species

We followed the methods used in previous modeling efforts for tamarisk and Russian olive in the western United States (Jarnevich and others, 2011; Jarnevich and Reynolds, 2010), updated with modeling methods being used to model cheatgrass distribution in the western United States (Morissette and others, 2013). Changes included incorporating updated location data from Global Invasive Species Information Network (www.gisinfo.org) and from BLM offices within the Wyoming basin, expanding the modeling techniques with the Software for Assisted Habitat Modeling (Morissette and others, 2013). Climate variables used in the model were derived from monthly averages of precipitation, minimum temperature, and maximum temperature for climate scenario II (Geophysical Fluid Dynamics Laboratory’s Coupled Climate model 2.1, emissions scenario A2) (Maurer and others, 2007). Models were developed using the standard Software for Assisted Habitat Modeling (SAHM) workflow for presence-only data (SAHM tutorial node “Presence only using the entire study area”).

We selected predictors based on previous models for the species (Jarnevich and Reynolds, 2010; Jarnevich and others, 2011) and variables useful for projecting future climates, removing nonclimate

predictors for which projections do not exist. We did retain distance to water (fine-resolution layer from Jarnevich and Reynolds [2010]), as this variable was an important predictor for both tamarisk and Russian olive in previous models. We used seven bioclimatic variables for the cheatgrass models and an additional two bioclimatic variables and distance to water for tamarisk and Russian olive (table A–17). Bioclimatic variables were derived following O’Donnell and Ignizio (2012) using Parameter-elevation Regressions on Independent Slopes Model (PRISM) climate averages for 1971–2000 and PRISM climate averages for 1980–2009. We used baseline climate data for the current models to examine the uncertainty associated with the baseline climate data used to train the model (Roubicek and others, 2010), and the differences may be exacerbated when projecting to future climate scenarios.

Area under curve (AUC) values from the spatial cross-validation were similar across model algorithms, so we selected the generalized linear models because they were the simplest models, which is beneficial for forecasting (Jiménez-Valverde and others, 2011)). These models are correlative based, and projections assume that correlations between predictors now are maintained in the future (Elith and others, 2010). The models also assume that species are in equilibrium with climate, but other factors could limit their distribution, such biotic interactions that may limit their distribution.

Table A–17. Climate variables used in the tamarisk and Russian olive distribution models, including values for their percent contribution to the model using climate data from 1971–2000 and 1980–2009, calculated by permutating the values at presence and background locations and calculating the change in area under curve (AUC). Empty cells indicate the predictor variables were not included as inputs into the model for that species.

Climate variable	Percent contribution to the model					
	Cheatgrass		Tamarisk		Russian olive	
	1971–2000	1980–2009	1971–2000	1980–2009	1971–2000	1980–2009
Mean diurnal range (Mean of monthly (max temp – min temp))	—	—	2.0	6.0	4.0	7.0
Temperature seasonality	3.0	4.0	1.0	5.0	3.0	4.0
Maximum temperature of warmest month	10.0	11.0	21.0	27.0	30.0	32.0
Minimum temperature of coldest month	54.0	62.0	38.0	38.0	34.0	34.0
Mean temperature of wettest quarter	—	—	7.0	7.0	4.0	9.0
Precipitation of driest month	—	—	1.0	0.2	11.0	2.0
Precipitation seasonality (coefficient of variation)	22.0	15.0	0	0.1	0	0
Precipitation of warmest quarter	5.0	5.0	24.0	13.0	10.0	5.0
Precipitation of coldest quarter	7.0	4.0	0.1	0.04	1.0	1.0
Distance to water	—	—	5.0	3.0	4.0	4.0

Landscape Structure: Terrestrial Structural Connectivity Analysis

To evaluate structural connectivity, we first evaluated the interpatch distances at which discontinuities in patch connectedness occurred for the mapped distribution of species and communities (hereafter distribution). Pronounced thresholds can indicate large discontinuities in the distribution of patches at particular spatial scales (see Chapter 2– Assessment Framework). This technique simplifies the complexity of multiscale spatial heterogeneity for analysis purposes, which allows us to compare the differences in the interpatch distances between baseline and relatively undeveloped areas to evaluate how development has potentially fragmented communities and habitats.

We conducted this analysis for both baseline conditions and relatively undeveloped areas (TDI ≤ 1 percent). Discontinuities were indicated by large increases in the maximum size of patch complexes (as a function of the total percent of the baseline distribution or relatively undeveloped areas) (figs. A–10 to A–13). These discontinuities were used as an index of local, landscape, and regional levels of patch connectedness and were used to identify the characteristic scales corresponding to each level of patch connectedness for a given species or community. The use of discontinuities in connectedness provides a process for selecting three scales at which to evaluate structural connectivity for baseline and relatively undeveloped areas. The three scales selected using this process, however, are not the only scales that may be relevant to a particular management question.

We used an upper threshold of 90 percent of the total area for the baseline or relatively undeveloped areas to identify thresholds that correspond to regional levels of connectivity. In a few cases, there were multiple small thresholds indicating that heterogeneity varied continuously across spatial levels. In these cases, we selected the most pronounced thresholds for identifying interpatch distances corresponding to each level of connectivity. The interpatch distances corresponding to local-, landscape-, and regional-levels of connectivity for baseline and relatively undeveloped areas are summarized for each species in table A–18.

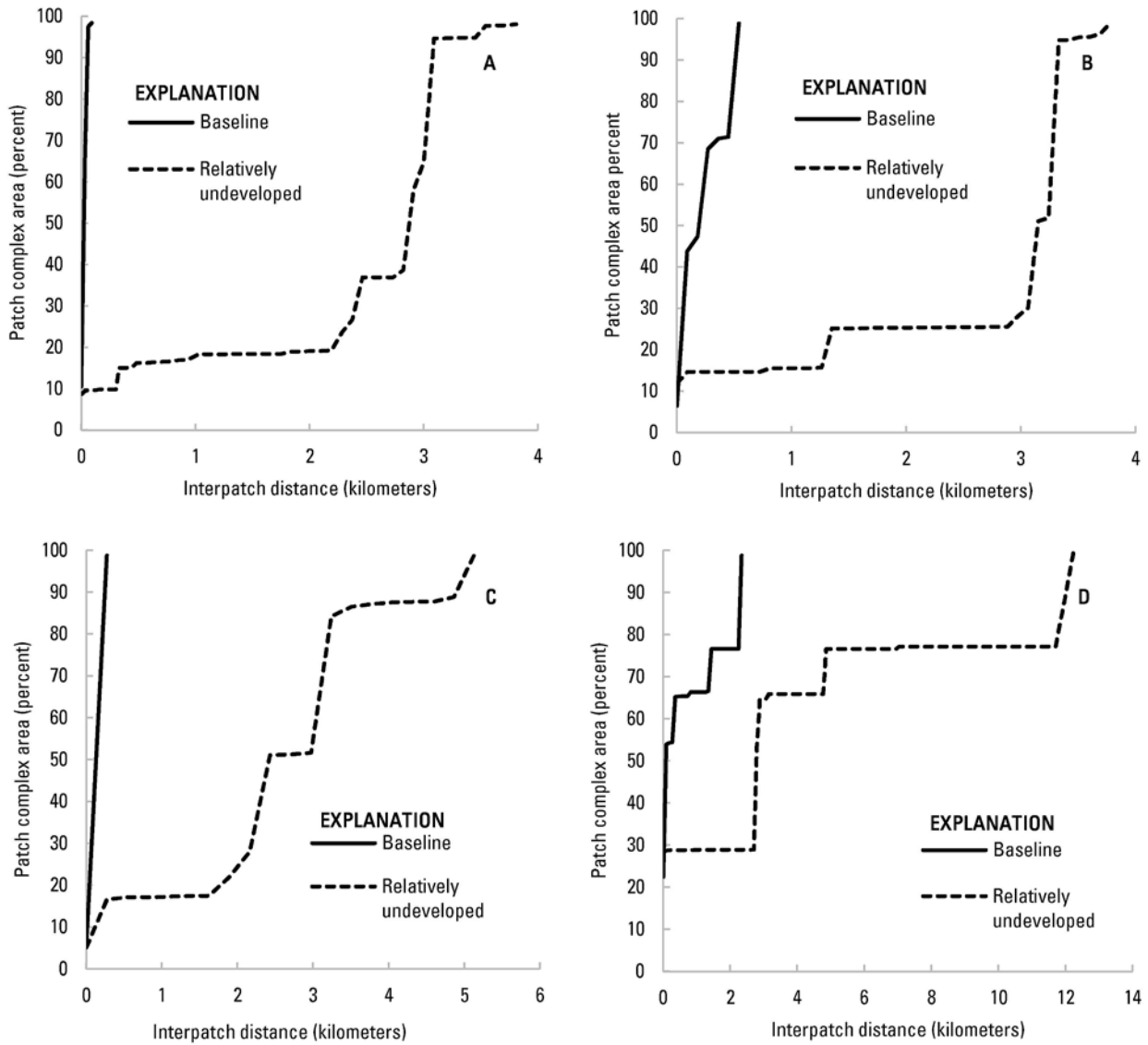


Figure A-10. Connectivity analysis for determining local, landscape, and regional levels of structural connectivity for the Wyoming Basin Rapid Ecoregional Assessment. (A) Sagebrush steppe, (B) desert shrublands, (C) foothill shrublands and woodlands, and (D) mountain forests and alpine zones.

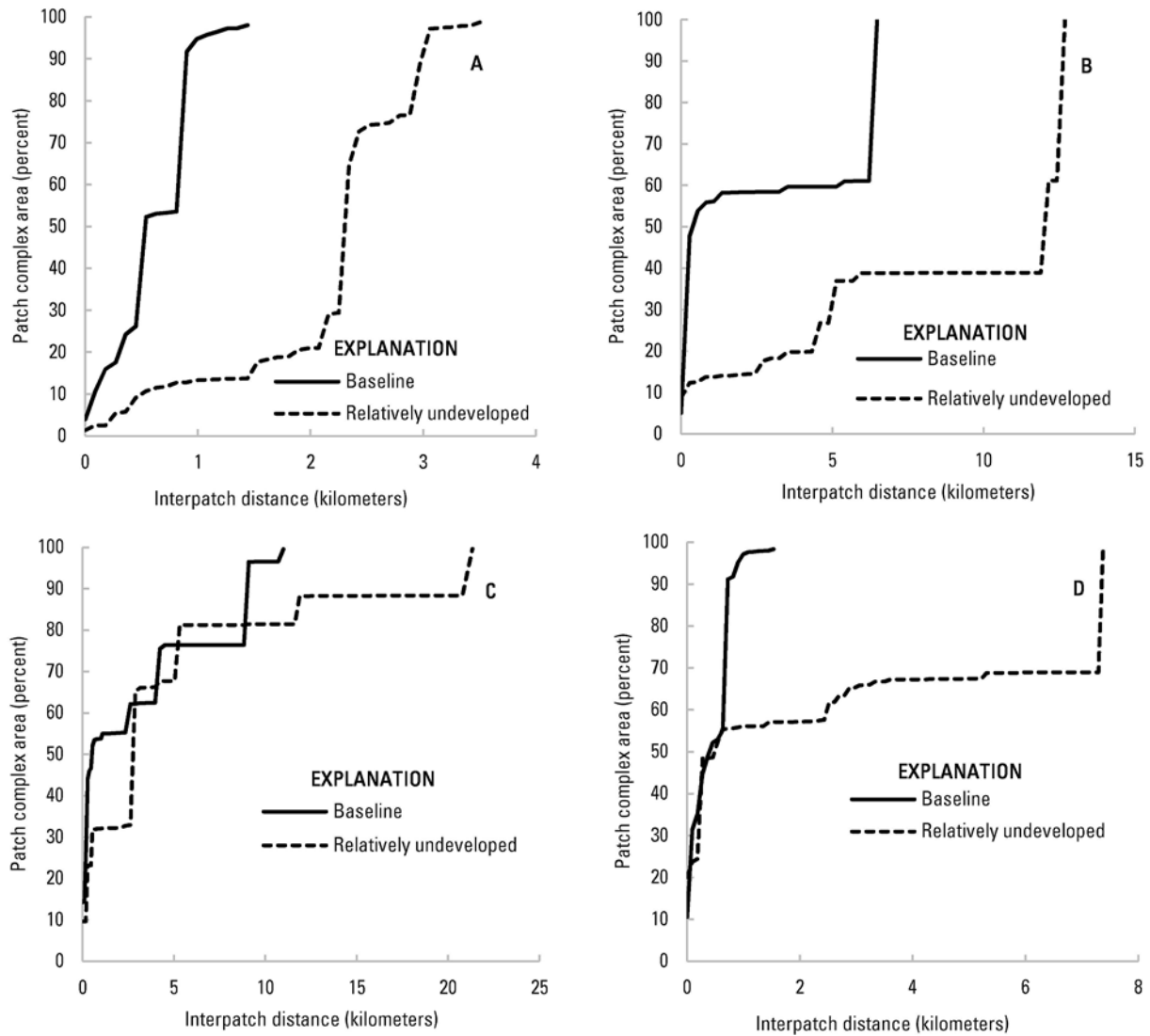


Figure A-11. Connectivity analysis for determining local, landscape, and regional levels of structural connectivity for the Wyoming Basin Rapid Ecoregional Assessment. (A) Wetlands, (B) aspen, (C) five-needle pine forests and woodlands, and (D) juniper woodlands.

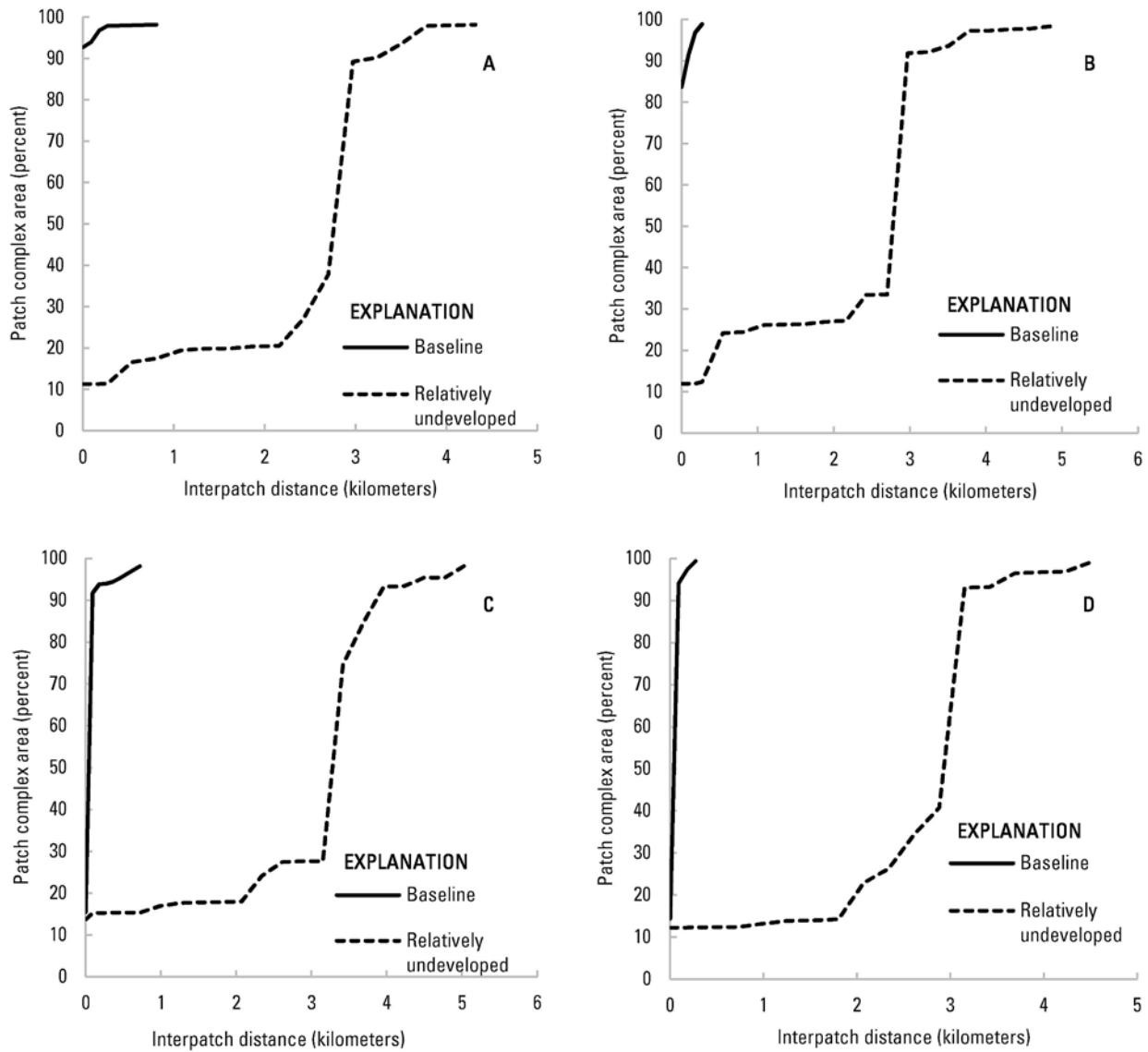


Figure A-12. Connectivity analysis for determining local, landscape, and regional levels of structural connectivity for the Wyoming Basin Rapid Ecoregional Assessment. (A) Greater sage-grouse, (B) golden eagle, (C) ferruginous hawk, and (D) sagebrush-obligate birds.

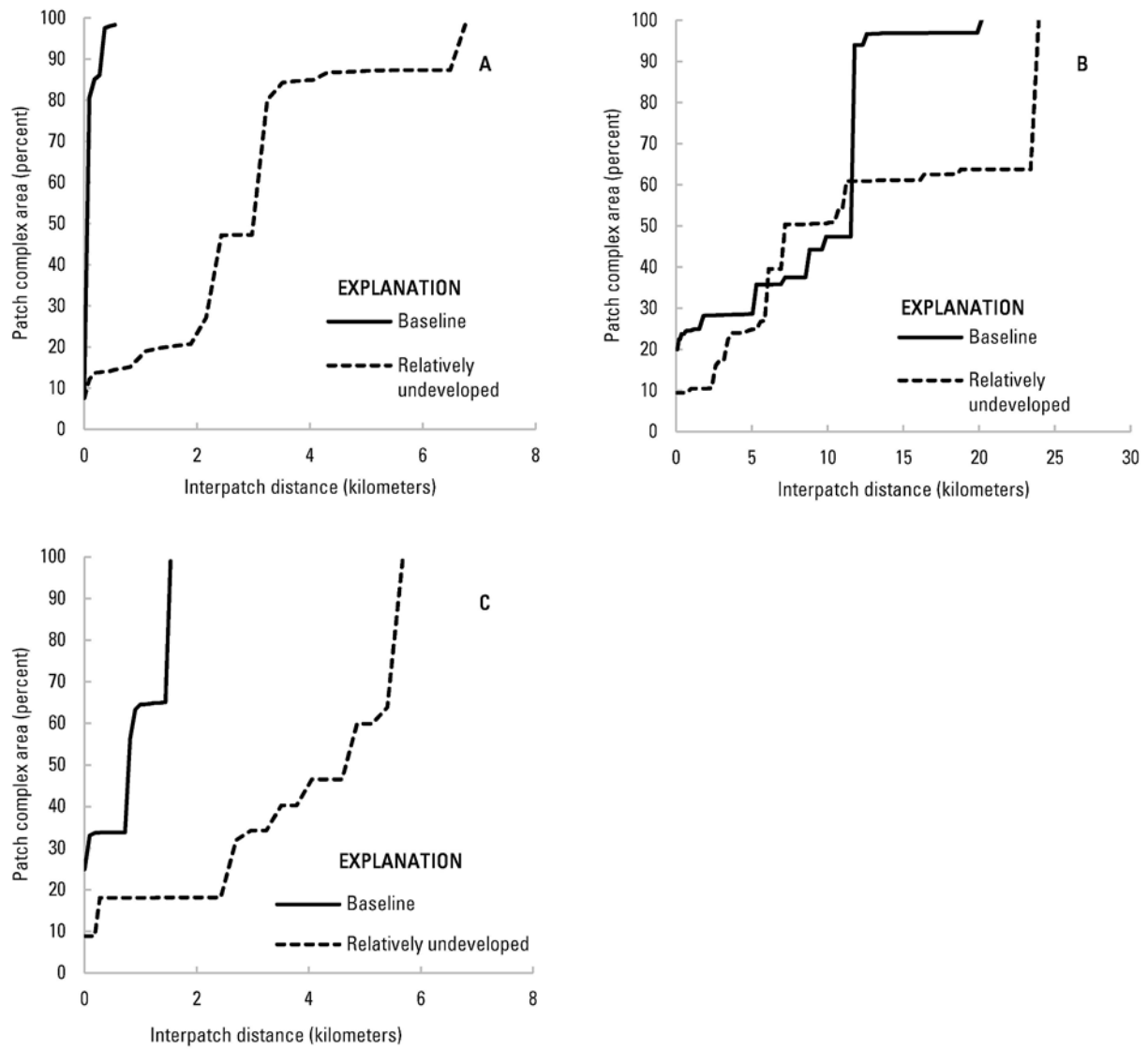


Figure A-13. Connectivity analysis for determining local, landscape, and regional levels of structural connectivity for the Wyoming Basin Rapid Ecoregional Assessment. (A) Pygmy rabbit, (B) mule deer crucial winter range, and (C) spadefoot assemblage.

Table A-18. Summary of interpatch distances corresponding to connectivity at local, landscape, and regional levels for baseline conditions and relatively undeveloped areas for terrestrial Conservation Elements evaluated for the Wyoming Basin Rapid Ecoregional Assessment.

[km, kilometer]

Conservation Element	Interpatch distance (km)					
	Connectivity level for baseline conditions			Connectivity level for relatively undeveloped areas		
	Local	Landscape	Regional	Local	Landscape	Regional
Sagebrush steppe	0.06	0.06	0.06	0.45	2.46	3.18
Desert shrublands	0.09	0.24	0.54	1.35	3.15	3.33
Foothill shrublands and woodlands	0.27	0.27	0.27	0.27	2.43	3.24
Mountain forests and alpine zone	0.36	1.44	2.43	3.15	4.86	12.24
Aspen	0.27	1.35	6.48	0.27	5.13	12.69
Five-needle pine	1.08	4.50	9.09	2.97	5.13	11.88
Juniper woodlands	0.45	0.72	1.08	0.63	3.33	7.38
Spadefoot assemblage	0.09	0.99	1.53	0.27	3.51	5.67
Greater sage-grouse	0.27	0.27	0.27	0.27	2.97	3.78
Golden eagle	0.09	0.18	0.18	0.54	2.97	4.86
Ferruginous hawk	0.09	0.09	0.09	1.26	3.96	5.04
Sagebrush-obligate birds	0.09	0.27	0.27	2.07	3.15	3.69
Pygmy rabbit	0.09	0.18	0.36	2.43	4.32	6.75
Mule deer crucial winter range	1.80	11.79	20.16	7.20	11.52	23.94
Wetlands	0.18	0.54	1.4	0.81	1.44	3.50

Integrated Management Questions

Integrated Management Questions summarize landscape-level ecological values (for key ecological attributes such as habitat area) and risks (from Change Agents such as development) derived from Core Management Questions. The combined ranks for landscape-level values and risks were used to rank the conservation potential of modeled distributions or mapped occurrences of species and communities. This approach summarizes information in a format that can be used as a screening tool for identifying areas with high conservation, restoration, or development potential. Values, risks, and conservation potential for terrestrial Conservation Elements were summarized by township 93.3 km² (36 mi²) and by fifth-level watershed for aquatic Conservation Elements.

We developed the following process for establishing breakpoints for ranking variables representing values and risks for each species and community. If available, we used published literature that provided a quantitative basis for breakpoints at the appropriate spatial scale. For example, the percent of greater sage-grouse habitat in a 78.5-km² (30.3 mi²) radius analysis unit (Knick and others, 2013) corresponded most closely to the township scale. In most cases, however, published information was not available to establish breakpoints.

For species lacking established breakpoints from published literature, we initially used equal subsets of each dataset (quantiles) to establish breakpoints. In many cases, the distribution of scores was highly skewed toward very low area scores, which resulted in breakpoints that were not biologically

meaningful or useful for identifying conservation potential. We also evaluated the use of equal breakpoints, natural breaks, and biologically meaningful breaks, but no single approach could be applied because of the differences in the distribution of scores for each variable and each Conservation Element. Thus, we examined the distribution of scores for each value and risk variable to determine the most appropriate method for establishing breakpoints. The technique used to create breakpoints for each variable is provided in table A–19.

For ranking the area of communities or habitats per township, we established a minimum area threshold to prevent townships with very limited area, which may result from mapping errors, from having a strong influence on the rank breakpoints. For most species and communities, this threshold was 1 percent of the township area (94 ha; 232 ac). For several species (juniper woodlands, and five-needle pine), we used a 0.1 percent minimum area threshold because there were often small isolated patches that occurred in some townships. Often, the townships above the minimum area threshold still had highly skewed scores for habitat or community area; consequently we established the breakpoints for equal subsets of the datasets for scores >2 percent of township area, but included the townships with 1–2 percent area in the lowest rank category (referred to as skew correction). For rivers and streams and for the fish species, we established a lower threshold of 10 m for stream segment length per fifth-level watershed to minimize the effects of mapping imprecisions.

For values or risks that were derived from ranked variables (such as the mean risk for sudden aspen decline per township), we used equal breakpoints. If the distribution had natural breaks that resulted in fairly equal subsets, we used natural breaks. In a few cases (such as lek proximity for greater sage-grouse), the distribution was bimodal, and we used biologically meaningful breaks to represent both ends and the middle of the distribution (for example, <20 percent, 20–80 percent, and >80 percent) to avoid combining scores that were very different into one rank.

The TDI score was used to assess risk for terrestrial species and communities, and the ADI was used to assess risk for aquatic species and communities. We establish standard breakpoints for ranking TDI and ADI, which were used to rank risks from exposure to development for each species and community (table A–19). Because the landscape-level value and risk maps were used to identify potential areas for conservation, we emphasized low development scores for ranking low and moderate risks.

If more than one value or risk variable was used, the overall landscape-level values and risks combined the ranks for each variable. We established breakpoints in the summed overall conservation potential ranks that resulted in the most even distribution in the number of townships among ranks (fig. 2–19). Landscape-level values and risks, and conservation potential rankings are intended to provide a synthetic overview of the geospatial datasets developed to address core Management Questions in the REA. Because rankings are very sensitive to the input data used and the criteria used to develop the ranking thresholds, they are not intended as stand-alone maps. Rather, they are best used as an initial screening tool to compare regional rankings in conjunction with the geospatial data for core Management Questions and information on local conditions that cannot be determined from regional REA maps.

Table A-19. Summary of variables used to address landscape-level values and risks for each Conservation Element. Green shading denotes variables representing landscape-level values, whereas orange shading denotes variables represent landscape-level risks.

[<, less than; >, greater than; TDI, Terrestrial Development Index; km, kilometer; ADI, Aquatic Development Index; ≥, greater than or equal to; km, kilometer; km², square kilometer; ha, hectare]

Conservation Element	Variable type	Variable	Lowest ranks	Medium ranks	Highest ranks	Breakpoint criteria
Aspen	Value	Area (percent of township)	<0.19	0.19–3.24	>3.24	Equal-sized data subsets
		Stepping stones	Local, landscape, and regional connectivity	Landscape and regional connectivity	Regional connectivity	Natural breaks
Aspen	Overall value	Maximum value rank	2–3	4	5–6	Equal-sized data subsets
Aspen	Risk	TDI	0–1	1–3	>3	Standard breaks
		Edge effect	>10 percent core area	1–10 percent core area	0–1 percent core area	Biologically meaningful breaks
		Sudden aspen decline	1–1.67	1.67–2.34	2.34–3	Equal intervals of ranks of high (3) or low (1) risk
Aspen	Overall risk	Average risk rank	3–5	6–8	9	Equal-sized data subsets
Cutthroat trout	Value	Mean fragment length (km)	<17	17–40	≥40	Equal-sized data subsets
		Segment count	0	1–3	4–34	Biologically meaningful breaks
		Lake count	0	1	2–8	Biologically meaningful breaks
Cutthroat trout	Overall value	Maximum value rank	3–4	5–6	7–9	Equal-sized data subsets
Cutthroat trout	Risk	ADI	0–20	20–40	>40	Standard breaks
		Number of zero mean summer flow segments /	0	0–0.080	≥0.080	Equal-sized data subsets
		Hybridization status and risk index	1	1.5–2	2.5–3	Biologically meaningful breaks
Cutthroat trout	Overall risk	Maximum risk rank	3–4	5–6	7–9	Equal-sized data subsets
Desert shrublands	Overall value	Area (percent of township)	<6	6–18	≥18	Equal-sized data subsets ¹

Conservation Element	Variable type	Variable	Lowest ranks	Medium ranks	Highest ranks	Breakpoint criteria
Desert shrublands	Overall risk	TDI	0–1	1–3	>3	Standard
Ferruginous hawk	Overall value	Area (percent of township)	<31	31–74	≥74	Equal-sized data subsets ¹
Ferruginous hawk	Overall risk	TDI	0–1	1–3	>3	Standard
Three-fish assemblage	Value	Mean segments length (km)	<31	31–66	≥66	Equal-sized data subsets
		Count of segments	0	1	2–3	Natural breaks
		Count of lakes	0	1	2–3	Natural breaks
Three-fish assemblage	Overall value	Maximum value rank	3–4	5–6	7–9	Equal-sized data subsets
Three-fish assemblage	Risk	ADI	0–20	20–40	>40	Standard
		Invasive species present (percent of watershed)	<20	20–80	≥80	Natural breaks
Three-fish assemblage	Overall risk	Average risk ranks	2–3	4–5	6	Equal-sized data subsets
Five-needle pine	Overall value	Area (percent of township)	<2.75	2.75–19.9	≥19.9	Equal-sized data subsets ²
Five-needle pine	Overall risk	TDI	0–1	1–3	>3	Standard
Foothill shrublands and woodlands	Overall value	Area (percent of township)	<11	11–34	≥34	Equal-sized data subsets ¹
Foothill shrublands and woodlands	Overall risk	TDI	0–1	1–3	>3	Standard
Golden eagle	Overall Value	Area (percent of township)	<33	33–79	≥79	Equal-sized data subsets ¹
Golden eagle	Overall risk	TDI	0–1	1–3	>3	Standard
Juniper woodlands	Overall value	Area (percent of township)	<0.36	0.36–1.38	≥1.38	Equal-sized data subsets ²
Juniper woodlands	Overall risk	TDI	0–1	1–3	>3	Standard

Conservation Element	Variable type	Variable	Lowest ranks	Medium ranks	Highest ranks	Breakpoint criteria
Leatherside Chub	Overall value	Percent of catchments occupied	<1.95	1.95–8.61	≥8.61	Equal-sized data subsets
Leatherside Chub	Overall risk	ADI	0–20	20–40	≥40	Equal-sized data subsets
Mountain forests	Overall value	Area (percent of township)	<26	26–76	≥76	Equal-sized data subsets ¹
Mountain forests	Overall risk	TDI	0–1	1–3	>3	Standard
Mule deer	Overall value	Area - crucial winter range	<17	17–49	>49	Equal-sized data subsets
Mule deer	Overall risk	TDI	0–1	1–3	>3	Standard
Pygmy rabbit	Overall value	Area (percent of township)	<9	9–45	≥45	Equal-sized data subsets ¹
Pygmy rabbit	Overall risk	TDI	0–1	1–3	>3	Standard
Riparian	Overall value	Area (ha/km ²)	68	69–75	>75	Equal-sized data subsets ²
Riparian	Risk	ADI	<20	20–40	≥40	Standard
		Number of dams	0	1–3	4–27	Low= 0; >0 natural breaks
		Presence/absence of invasive species	1	2	3	Based on Bureau of Land Management and LANDFIRE data ³
Riparian	Overall risk	Average risk rank	3–4	5–6	7–9	Equal-sized data subsets
Sage-grouse	Value	Area (percent of township)	0–0.35	0.35–0.79	<0.79	Biologically meaningful breaks derived from the literature (Knick and others, 2013)
		Proximity to lek	<20	20–80	>80	Biological meaningful breaks
Sage-grouse	Overall value	Average value rank	2–3	4	5–6	Equal-sized data subsets
Sage-grouse	Risk	TDI	0–1	1–3	>3	Standard
Sagebrush obligate songbirds	Overall value	Area (percent of township)	<48.8	48.8–91.9	>91.9	Equal-sized data subsets ¹

Conservation Element	Variable type	Variable	Lowest ranks	Medium ranks	Highest ranks	Breakpoint criteria
Sagebrush obligate songbirds	Overall risk	TDI	0–1	1–3	>3	Standard
Sagebrush steppe	Overall value	Area (percent of township)	<44	44–75	≥75	Equal-sized data subsets ¹
Sagebrush steppe	Overall risk	TDI	0–1	1–3	>3	Standard
Sauger	Value	Mean segment length (km)	<22	22–40	≥40	Equal-sized data subsets
		Segment count by fifth-level watershed	0	1	2–3	Low = 0; >0 equal-sized data subsets for remaining distribution for medium and high
		Lake count by fifth-level watershed	0	1	2–5	Natural breaks
Sauger	Overall value	Maximum value rank	3–4	5–6	7–8	Sauger
Sauger	Risk	ADI	<20	20–40	≥40	Standard
		Number of zero mean summer flow segments	0	0–0.5	≥0.5	Low risk = 0; >0 equal-sized data subsets for medium and high
		Invasive species (% of catchments with walleye present)	<37	37–78	>78	Natural breaks
Sauger	Overall Risk	Average risk rank	3–4	5–7	8–9	Equal-sized data subsets
Spadefoot assemblage	Overall value	Area (percent of township)	<6	6–22	≥22	Equal-sized data subsets ²
Spadefoot assemblage	Overall risk	TDI	0–1	1–3	>3	Standard

Conservation Element	Variable type	Variable	Lowest ranks	Medium ranks	Highest ranks	Breakpoint criteria
Streams and rivers	Value	Perennial stream density (length:area ratio [km/km ²])	<0.13	0.13–0.34	≥0.34	Equal-sized data subsets
		Ephemeral stream density (length:area ratio [km/km ²])	<1.12	1.12–1.56	≥1.56	Equal-sized data subsets
Streams and rivers	Overall value	Sum of rank values	2–3	4	5–6	Equal-sized data subsets
Streams and rivers	Risk	ADI	<20	20–40	≥40	Standard
		Number of dams	0	1–2	>2	Low = 0; >0 equal-sized data subsets for remaining distribution for medium and high
Streams and rivers	Overall risk	Average risk rank	2–3	4	5–6	Equal-sized data subsets
Wetlands	Overall value	Area	<1percent	1–3 percent	≥3–23percent	Equal-sized data subsets
Wetlands	Overall risk	Local ADI	<20	20–40	≥40	Standard

¹ We used a lower threshold of 1 percent of the township area. In addition, skew corrections were made as follows: juniper (0.1 percent); pygmy rabbit (1 percent); and desert shrublands, ferruginous hawk, foothill shrublands and woodlands, golden eagle, juniper woodlands, mountain forest, sagebrush obligated songbirds, and sagebrush steppe (2 percent).

² For spadefoot assemblage, we used a lower threshold of 0.01 percent of the township area with a skew correction of 1 percent. For juniper woodlands and five-needle pine, we used a lower threshold of 0.1 percent of the township area with a skew correction of 2 percent.

³ For riparian zone risk of invasive species: if known occurrences of invasive species (derived from Bureau of Land Management data), the rank was highest; if LANDFIRE indicated invasive species were present, the rank was medium; otherwise, the rank was lowest.

Wildland Fire

Fire occurrence data were compiled from U.S. Department of Agriculture Forest Service, U.S. Geological Survey (GeoMac), National Park Service (Monitoring Trends in Burn Severity), Bureau of Land Management, and National Fire and Aviation Management Web applications.

At the coarse scales of Bailey's ecoregions (Bailey 1995), the subregional differences in fuels can be masked by regional relationships that are "averaged" over large areas. Littell and others (2010) and Littell and Gwozdz (2011) introduced fire-climate regression models for Bailey's ecoregions, the next finer classification in the Bailey system, for the Pacific Northwest (Columbia Basin and western Montana). These finer resolution models had similar fuels sensitivities but at finer scales. For example, variability in fire area in forested systems was primarily related to climate variables associated with lower than normal fuel moisture such as increased summer temperature, decreased summer precipitation, increased water balance deficit (potential minus actual evapotranspiration), increased vapor pressure deficit, decreased soil moisture, and other hydrologic variables. In contrast, variability in fire area in nonforested systems was negatively related to variables affecting fuel moisture and antecedent variables affecting vegetation productivity and possibly fuel continuity, such as increased precipitation and decreased temperature.

The hydrologic output required to assess the relationship between fire and climate for the Wyoming Basin ecoregion was developed by Littell and others (2011) following methods in Elsner and others (2010). Briefly, monthly gridded historical climate (temperature, precipitation, wind) averages or totals were developed for approximately 36-km² (13.9-mi²) cells across the Columbia, upper Missouri, and upper Colorado River basins for the period 1916–2006. These variables were combined with local topographic, vegetation and soil parameters in the Variable Infiltration Capacity hydrologic model to estimate approximately 20 derived hydrologic variables (including potential evapotranspiration, actual evapotranspiration, vapor pressure deficit, snow water equivalent, soil moisture, and relative humidity). In this analysis, we chose to use climatic and hydrologic variables that have been commonly hypothesized or shown to be related to fire activity, including temperature, precipitation, soil moisture, snow pack (estimated by snow water equivalent), relative humidity, vapor pressure deficit, potential evapotranspiration (PET), and actual evapotranspiration (AET). In addition, we used combinations of these variables that try to capture the hydrologic or ecological mechanisms responsible for fuel availability, including combined flow (runoff + baseflow, an index of total water availability), water balance deficit (PET - AET), a form of climatic water deficit (precipitation - PET), and water balance deficit and climatic water deficit normalized by PET. Further details, including correlations with monthly and (or) seasonal variables are in (figs. 5-1 to 5-4).

We followed methods in Littell and others (2010) and Littell and Gwozdz (2011) and aggregated area burned observations using administrative unit from the National Interagency Fire Management Integrated Database. We evaluated the area burned between 1980–2006 for duplicate observations and other obvious attribution errors, and quantified the area burned by ecoregion using percentage area (U.S. Department of Agriculture Forest Service, National Park Service, U.S. Fish and Wildlife Service, BLM, and Bureau of Indian Affairs protected areas). Characteristics of the distribution of area burned are presented in table 5-3. Most of the fire occurrences were dominated by low annual area burned and a few years with high area burned.

We then developed regressions of area burned as a function of climate (table A-20). We used Pearson correlations between the time series of log-transformed hectares burned and the time series of available monthly and seasonal climate variables for the common period, 1980–2006. In addition, we considered climate in the two years prior to the observed fire season, similar to Littell and others (2009).

In such a strategy, there are numerous possible climate predictors, many of which are sufficiently correlated with each other, such that choices among them are essentially arbitrary because either would produce a similarly skilled regression. We prioritized year-of-fire relationships unless lagged relationships were clearly better predictors (better correlations and in-regression performance), and we also prioritized seasonal aggregations of several months with similar correlations over single-month relationships that could be spurious and merely the consequence of running many correlations. We entered the highest correlating variables into regression models first, retaining only those with $P(t) < 0.05$ and rejecting those with $P(t) > 0.1$. We built the models forward until the fit (measured by R^2) could not be improved further. To avoid possibly spurious projections and overfitting, we did not include interaction terms in the regressions, although it should be noted that such interactions can sometimes be used diagnostically to better understand the historical controls of climate on fire. We calculated Durbin-Watson tests for autocorrelation of residuals and considered predictors as autocorrelated if Variance Inflation Factor (VIF) statistics for a single variable exceeded 2.5.

Table A-20. Regression models representing historical fire-climate sensitivities and regression diagnostics. [Model parameter signs (positive or negative) are indicated in parentheses; “+” not in parentheses indicates that the regressions consider variables as additive; PET, evapotranspiration; potential AET, actual evapotranspiration; PPT, precipitation; Lag1, the year prior to the observed fire year; Lag2, two years prior to the observed fire year; VPD, vapor pressure deficit; and SWE, snow water equivalent; R^2 , r-squared; VIF, Variance Inflation Factor]

Ecosection	Model	R^2	VIF
Yellowstone Highlands	(+)July-Sept. PET – July-Sept. AET	0.86	NA
Bighorn Mountains	(-)June-Aug. PPT – July-Sept. PET + (+) Lag1 Oct. VPD +(-)Lag2 Oct.-Dec. PET1	0.73	1.00-1.17
Wind River Mountain	(+)July-Sept. VPD + (+)Lag2 June PPT	0.50	1.00-1.01
Bighorn Basin ¹	(+)July-Sept. PET1 + (-)Dec.-Feb. SWE + (-)Lag2 Dec.-Feb. SWE	0.55	1.06-1.08
Bear Lake	(+)Lag1 Nov. VPD	0.44	NA
Central Basin and Hills	(+)April-Sept. VPD + (-)Lag1 July-Sept. PET3 + (-)Lag2 Oct.-March SWE	0.66	1.06-1.09
Greater Green River	(+)July-Sept. PET – July-Sept. AET + (-)Lag1 July-Sept. PPT/ July-Sept. PET	0.43	1.00-1.00

¹ The Bighorn Basin model is marginally statistically significant ($p \geq 0.05$).

Relationships indicating climate facilitation of fire (for example, increased productivity or fuel production) generally were weak compared to variables indicating moisture limitation, and most models included primary terms related to hydrologic deficit, as represented by either the difference between potential and actual evapotranspiration (water balance deficit and PET – AET) or the difference between precipitation and potential evapotranspiration (a form of “climatic water deficit”). Vapor pressure deficit was important in several models, although the season and strength of the relationship varied with ecosection. Finally, snow water equivalent (SWE) in winters prior to the fire season was a secondary, negative predictor in the Bighorn Basin and Central Basin and Hills ecosections, indicating that some role of winter drought is evident independent of summer water demand.

Regression models used for future projections are described in table 5–4. We were able to develop acceptable models for all ecosections except the Bear Lake ecosection, which had a trend in residuals strong enough to result in questionable projections. In addition, the Bear Lake ecosection has only a handful of years with nonzero observations, making the correlations with lagged November VPD dubious. The Big Horn Basin ecosection also had some autocorrelation in its residuals, and although it passed the Durbin-Watson test, indications are the projections from this model may also underestimate the variability in area burned for years of high climatic fire potential. The regression model for the Central Basin and Hills ecosection also under-predicts historical observed area burned possibly because historical means were used as input for the lagged variables and the sequence of these variables may be a better predictor of area burned than the mean value.

We used future downscaled climate and hydrologic projections from Littell and others (2011) aggregated (averaged across cells) to the Bailey ecosection level. The mean climate variables for the 2040s (2030–2059) and 2080s (2070–2099) were available from the Littell and others (2011) work, and we used those values in the regression models (table 5–4) to project the expected area burned given the mean climate estimates. We developed projections for an ensemble of 10 global climate models (Bjerknes Centre for Climate Research [BCCR]; Centre National de Recherches Meteorologiques, Climate Model, ver. 3 [CNRM-CM3]; Commonwealth Scientific and Industrial Research Organisation, Centre for Australian Weather and Climate Research, climate model Mk3.5 [CSIRO3.5]; European Center Hamburg Model, ver. 5 [ECHAM5]; ECHO-G; Hadley Centre Climate Model [HADCM]; Hadley Centre Global Environmental Model, ver. 1 [HADGEM1]; Model for Interdisciplinary Research on Climate, ver. 3.2 [MIROC3.2]; Model for Interdisciplinary Research on Climate using High Resolution data [MIROC3.2, HI]; and National Center for Atmospheric Research, Parallel Climate Model, ver. 1 [PCM1]), as well as projections for four bracketing models (ECHAM5, HADGEM1, MIROC3.2, and PCM1), all for the Special Report on Emissions Scenarios A1B emissions scenario. Note that these projected values are derived from the mean future climate projected for the ecosections, and not the full range of variability encountered in the 20th and 21st centuries. Better estimates of the range of expected future fire responses could be developed by using interannual time series of future projections (which exist, but have not yet been aggregated to the scale of the fire data). This is particularly key for fire responses, which were nonlinearly distributed.

In most ecosections, increasing PET and VPD were responsible for the increase in area burned, and any changes in precipitation or AET were insufficient to counteract the increase in water deficit. In the Big Horn Basin and the Central Basin and Hills ecosections, projected increases in area burned also were related to projected decreases in winter snow. These relationships both point to increased fuel availability via flammability as the main mechanism for increased area burned. Future composite projections of mean area burned were clearly outside the modeled confidence intervals for the historical mean for the Yellowstone Highlands and Big Horn Mountains ecosections for the 2040s and 2080s and for the Big Horn Basin ecosection in the 2080s (table A–20). The MIROC3.2 global climate model (GCM), which projected warmer, drier summers in the northern U.S. Rocky Mountains, is the only model that exceeded this range in the 2080s for the Central Basin and Hills and Greater Green River Basin ecosections.

Table A–21. Projections of mean area burned for the 2080s.

[All areas were rounded to the nearest whole number; ha, hectare; ECHAM5, European Center Hamburg Model, version 5; HADGEM1, Hadley Centre Global Environment Model, version 1; MIROC3.2, Model for Interdisciplinary Research On Climate, version 3.2 (University of Tokyo); and PCM1, Parallel Climate Model version 1 (National Center for Atmospheric Research).]

Ecosection	Historical (modeled) (ha)	2080s A1B (ha)				
		Ensemble	ECHAM5	HADGEM1	MIROC3.2	PCM1
Yellowstone Highlands	169	4,792	425	17,790	60,053	1,229
Big Horn Mountains	21	12	5	10	20	13
Wind River Mountain	5	183	58	198	1,158	53
Big Horn Basin	185	1,085	842	1,605	946	798
Central Basin and Hills	27	632	450	1,962	1,125	200
Greater Green River Basin	355	633	420	289	2,355	547

Climate Analysis

Current Climate—Observations and Analysis

Data for defining the recent history of climate were from gridded observational datasets from weather stations dating back to the late 1800s, that became the National Oceanic and Atmospheric Administration National Weather Service Cooperative Observer Network (also known as the COOP network), and a special climate observing network, the Climate Reference Network of the National Oceanic and Atmospheric Administration National Climatic Data Center; see COOP observation stations in Wyoming at <http://www.ncdc.noaa.gov/oa/climate/uscrn/>. The Snow Telemetry (SNOTEL) network, operated by the U.S. Department of Agriculture National Resources Conservation Service, is a west-wide system for obtaining snow and other weather and hydrologic measurements at higher elevations; see SNOTEL observation stations around the Wyoming Basin at <http://www.wrds.uwyo.edu/wrds/nrcs/SnowDataSitesFront.pdf>. The distribution of stations in Wyoming is illustrative of stations in the Wyoming Basin in adjacent states, with COOP stations generally at elevations below 2,500 m (8,200 ft) and SNOTEL stations at higher elevations.

Because observation stations are not evenly distributed, a standard practice is to construct gridded observational datasets, which interpolate between stations using statistical models to account for elevation and terrain. In Chapter 7—Climate Analysis, figures 7–1 to 7–3 used these gridded observed datasets. Gridded datasets used directly in this report or by studies cited herein include the following.

- The PRISM gridded observational dataset (Di Luzio and others, 2008) gathers observations from a wide range of monitoring networks and uses statistical models that account for elevation, slope and aspect to interpolate among stations to develop spatially gridded climate datasets for the study of short- and long-term climate patterns (<http://www.prism.oregonstate.edu/>). The PRISM data used in this report were at a resolution of 4 km (2.5 mi).
- The Bias-Corrected Spatially Downscaled (BCSD) gridded observational dataset (Maurer and others, 2007) uses an interpolation methodology similar to PRISM to create a dataset with gridboxes 1/8° latitude-longitude (about 12 km [7.5 mi] at Wyoming Basin’s latitude) dataset, which is used in the analysis of the BCSD projections data (http://gdodcp.ucllnl.org/downscaled_cmip_projections/).

We compared BCSD and the Rehfeldt gridded observations and found them to be similar given the difference in resolution.

- Rehfeldt and others (2006) developed a gridded observational dataset for use in their vegetation modeling work. Their “thin spline” interpolation method accounts for spatially varying elevation relationships (Daly and others, 2008), and is similar to the method used to generate the WorldClim dataset that is widely used by ecologists (Hijmans and others, 2005). However, in the approach used by Rehfeldt and others (2006), the polynomials act as a smoothing function and do not handle sharp gradients, such as those in mountainous regions or areas with strong temperature inversions (Daly, 2008). Most of the Wyoming Basin is fairly flat, except the surrounding mountains; thus, the Rehfeldt downscaling is likely to adequately represent precipitation and temperature of the valley areas, assuming the input observations are reasonable.

We compared the Rehfeldt gridded observational datasets to the BCSD and PRISM datasets for the Wyoming Basin (not shown), and found them to be very similar, given the slightly different resolutions, and similar enough given the broad scales of the REA. We concluded that the Rehfeldt product was a reasonable choice for the REA analysis.

Future Climate—Projections Methods and Datasets

Choice of CMIP3 Generation of Models

In 2013, the Intergovernmental Panel on Climate Change fifth assessment (Intergovernmental Panel on Climate Change, 2013) provided a new generation of climate-projection models (the Coupled Model Intercomparison project Phase 5 [CMIP5]). When the Wyoming Basin REA was initiated, however, CMIP5 output was only just becoming available, and few analyses of these models were available in the published literature. The CMIP5 models do offer some enhancements, such as improved representation of the characteristic 2- to 7-year timescale for recurrence of El Niño Southern Oscillation (Intergovernmental Panel on Climate Change, 2013; Sheffield and others, 2013). Seager and others (2012) conducted a study of surface water availability projected by CMIP5 models for North America, including the Wyoming Basin. Similar to the CMIP3 results described in Chapter 7—Climate Analysis, they found that, for the 2021–2040 period, the CMIP5 projected a shift to wetter conditions (compared to 1951–2000) in the fall (October–November) and winter (January–March). For April–June and July–September, they also found a north-to-south gradient in precipitation changes, with a projected increase in the north and a decrease in the south; however, precipitation minus evaporation ($P - E$, a variable related to soil moisture) was projected to decrease (become drier) than it has been for the current climate.

The overall result of a warming world, however, was not expected to be significantly different in CMIP5 compared to CMIP3, which has now been confirmed in published results (Knutti and Sedláček, 2012; Intergovernmental panel on Climate Change, 2013). The CMIP3 generation of models already captured many aspects of the seasonal movements of storm tracks over North America (Karl and others, 2008), which are a major feature of climate in Wyoming; the simulated storm tracks in CMIP5 are improved over CMIP3 but are still positioned a little too far south, are weaker, and show fewer storms than observed when measured in terms of atmospheric pressure variations (Chang and others, 2012). Sidebar 5–1 in Lukas and others (2014) provides a longer discussion of the differences as they relate to the interior West.

Given that the CMIP3 and CMIP5 results were similar overall, especially at the biome scale, the differences were within the range of reasonably foreseeable futures represented in the CMIP3

generation of models. Therefore, we chose to work with the 2007 generation of output, and the many ecological and hydrological studies that are derived from that output. The same choice was made for the National Climate Assessment, which was underway at the same time (Kunkel and others, 2013; Cayan and others, 2013; Gershunov and others, 2013); thus, the discussion in Chapter 7—Climate Analysis is a snapshot of the current state of climate understanding overall, as well as climate in the Wyoming Basin ecosystems.

The Global Context

The starting point for all climate projections analyzed for this report was the set of models run for the CMIP3. This included over 20 GCMs which were used to produce simulations of the past and projections of the future. Chapter 7—Climate Analysis focuses on projections from seven of these CMIP3 GCMs (CCCM3) and ensemble averages of up to 16 GCMs. The 20th-century simulations of all these models used the best estimates of the temporal variations in external forcings, such as solar output and concentrations of volcanic aerosols and greenhouse gases. The future projections assumed changes in greenhouse gas concentrations; we focused on the A2 emissions scenarios, as directed by the BLM.

Chapter 7—Climate Analysis describes the North American context for change in the Wyoming Basin, the multimodel mean for the CMIP3 models at their original resolution of 2–3° latitude-longitude or about 160–320 km (100–200 mi). Chapter 7—Climate Analysis references figure 5–1 in Ray and others (2008), which illustrates North American temperature and precipitation changes projected for 2050 (2040–2060 average), derived from the global analysis in the 4th Intergovernmental Panel on Climate Change report (fig. 11.12 in Intergovernmental Panel on Climate Change, 2007). Although this analysis used the A1B emissions scenario, the A1B, A2, and B1 emissions scenarios result in a similar range of global and regional climate change out to the mid-21st century, and thus for 25- and 50-year planning horizons, the implications of all three scenarios are similar; later in the 21st century, however, the scenarios diverge (p.18 in Ray and others, 2008; fig 2.23 in Walsh and others, 2014). The top two rows in figure 2.23 (Walsh and others, 2014) show the difference of the multimodel average for the period 2040–2060 from the average of the 20th-century model runs for the baseline period of 1950–1999.

Downscaling Products and Methods

The spatial resolution of most GCMs is 2–3° latitude-longitude or about 160–320 km (100–200 mi), which is too large for most policy and planning purposes. Therefore, the GCM output has been downscaled by a number of groups each using different strategies, described in more detail in Fowler and others (2007) and Barsugli and others (2012). However, no one downscaling product suited all the tasks, so we consulted the following products, including the Hostetler downscaling, as directed by BLM (table A–22 gives more details on each downscaling product).

Table A–22. Downscaled climate projection datasets for possible inclusion in climate analysis. Reclamation Bias-Corrected and Spatially Downscaled (BCSD) and Bias-Corrected Constructed Analog (BCCA; downscaled) datasets use two of the same general circulation models (National Oceanic and Atmospheric Administration Geophysical Fluid Dynamics Laboratory Climate Model, ver. 2, and European Center Hamburg Model, ver. 5) used in the U.S. Geological Survey dynamical downscaling; BCSD and BCCA downscaled more global climate models than indicated here—the ones shown in this table are only those used in common with U.S. Geological Survey and Shafer. Rehfeldt used some models in common with each of the other four downscaling efforts.

[km, kilometer; ECHAM5, European Center Hamburg Model, ver. 5; GCM, global climate model; GENMOM, Global Environmental and Ecological Simulation of Interactive Systems, ver. 3 combined with Modular Ocean Model, ver. 2; GFDL2.0 or 2.1, Geophysical Fluid Dynamics Laboratory Climate Model, ver. 2.0 or 2.1; SRES, Special Report on Emissions Scenarios; VIC, variable infiltration capacity]

	U.S. Geological Survey (Hostettler and others, 2011)	Rehfeldt	Bias-Corrected Spatial Disaggregation (BCSD)	Bias-Corrected Constructed Analog (BCCA)	Projections of future climate for resource management
Institution of origin	U.S. Geological Survey	U.S. Department of Agriculture Forest Service	Bureau of Reclamation /Lawrence Livermore National Laboratory	Bureau of Reclamation /Lawrence Livermore National Laboratory	Forest Service
Down-scaling method	Dynamical downscaling by regional climate model RegCM3 ¹	Statistical downscaling with interpolation and spline model	BCSD and post-processing with VIC hydrologic/ land surface model	BCCA and post-processing with VIC hydrologic/ land surface model	Statistical/ delta method with VIC hydrology model
Spatial resolution	15 km	1 km	About 12 km (1/8 degree)	About 12 km (1/8 degree)	~5 km (1/16 degree)
Temporal resolution	Daily, decadal, and monthly means for 1968–1999, 2040–2069, 2010–2099	Monthly, decadal means around 2030, 2060, 2090	Monthly means, 1950–2099	Daily 1961–2000, 2046–2065, 2081–2100	Monthly means for 2030–2059, aka 2040s, and 2070–2099, aka 2080s
International Panel on Climate Change SRES emissions scenarios downscaled	A2	B1, B2, A2 (varies for GCM used)	B1, A1B, A2	B1, A1B, A2	A1B
General circulation models downscaled	GFDL2.0 ² ECHAM5 ³ GENMOM ⁴	GFDL2.1 ²	GFDL2.0, 2.1 ECHAM5	GFDL2.0, 2.1 ECHAM5	

- Hostetler and others (2011) downscaled one run from each of 3 GCMs to drive their dynamical downscaling, which they chose because of the range of sensitivities of the GCM to greenhouse gas forcing: 2–4 °C for ECHAM and 3–5 °C for Geophysical Fluid Dynamics Laboratory Climate Model, ver. 2.0 (GFDL2.0). They also downscaled a third GCM, GENMOM (combines the Global Environmental and Ecological Simulation of Interactive Systems, ver. 3 atmospheric GCM with the Modular Ocean Model, ver. 2), which is not included in CMIP3 or 5 and was not downscaled by any of the other products. Note that according to the IPCC (2007), “climate sensitivity,” or the equilibrium temperature change in different GCMs in response to the same radiative forcing, is *likely* to be in the range of 2–4.5 °C with a best estimate of about 3 °C and is *very unlikely* to be less than 1.5 °C. Hostetler and others (2011) concluded that values substantially higher than 4.5 °C cannot be excluded, but agreement of models with observations is not as good for those values. The mean ± 1 standard deviation value from 18 GCMs in the fourth assessment was 3.26 °C \pm 0.69 °C (box 10.2 in IPCC, 2007).
- Rehfeldt and others (2012) developed a statistical downscaling for the U.S. Department of Agriculture Forest Service for ecological studies and subsequently used the output to drive ecological models for aspen and other species. They used a thin spline interpolation similar to the method used in the WorldClim downscaling widely used in the ecological community. The spatial resolution is 1-km (0.62-mi), and the dataset provides monthly averages of some daily variables (for example, monthly average of daily minimum temperature); decadal means around 2030, 2060, 2090 (for example, means of the modeled years 2025–2034, 2055–2064, and 2085–2094). This product includes one run each downscaled from each of five GCMs (see table A–22). Differences between model projections likely are larger than any errors introduced by downscaling.
- Bias-Corrected Spatially Downscaled dataset (BCSD) (Bureau of Reclamation 2013, 2011; Maurer and others, 2007)—Created to support hydrologic assessment by the Bureau of Reclamation over the Western United States, this product bias-corrected and spatially downscaled CMIP3 GCM projections (http://gdo-dcp.ucllnl.org/downscaled_cmip3_projections). In total, 112 climate projections from 16 GCMs, and several emissions scenarios, were translated into hydrologic projections using watershed applications of the Variable Infiltration Capacity (VIC) macroscale hydrology model (developed at the University of Washington). Outputs from the VIC models include snowpack and runoff distributed over the watershed. This product excluded about a third of the models in the CMIP3 archive, which their evaluation indicated was not performing as well. This left 16 GCMs, some of which were run multiple times, for a total of 36 runs that make up the ensemble we use in this report. The remaining spread of these 36 model runs might be thought of as representing the range of reasonably foreseeable futures.
- Two downscaled products in this report both use the “Projections of Future Climate for Resource Management” (Littell and others, 2011). The Western Stream Flow Metric Dataset (used in Chapter 18—Cutthroat Trout and Chapter 6—Terrestrial Invasive Plant Species) was downscaled for river basins. It uses the same techniques as BCSD but includes further post-processing to generate hydroclimate variables that affect biomes. In particular, this product calculated several hydroclimate variables relevant for fire, trout, and invasive species studies. A second product from the same downscaled projections dataset was downscaled to ecoregions and was used in Chapter 5—Wildland Fire. This product was downscaled to the 2040s and 2080s, including MIROC3.2 and PCM1 and a 10-GCM ensemble mean. This product used the A1B emissions scenario, which is not appreciably different from A2 until after mid-century (see fig 2.23 in Walsh and others, 2014).
- North American Regional Climate Change Assessment Program (NARCCAP)—Although we did not analyze this dynamical downscaling, we discuss the results of this downscaling as they were

analyzed in the National Climate Assessment, including the Great Plains chapter of which Wyoming is a part. This product downscaled 3 GCMs used by other products in this study (Canadian Centre for Climate Modeling and Analysis Coupled Global Model, ver. 3 [CCCMA], GFDL2.1, and Hadley Centre Climate Model, ver. 3 [HADCM3]).

- Hayhoe and others (2004, 2008)—Also statistically downscaled CMIP3 models, developing a product with daily data that is useful for looking at metrics like number of days of extreme temperatures. Like NARCCAP, this product was used in the National Climate Assessment, and we discuss these results for the Wyoming Basin in the Climate chapter sections on other temperature and precipitation variables.

Comparison and Strengths and Weaknesses of Downscaling Products

The BLM directed that the report consider the dynamical downscaling done by Hostetler and others (2011). Few ecological studies, however, had been done using this product, in contrast to the body of published work using the Rehfeldt, BCSO, and the Western Streamflow products. Ecologists exploring the use of the Hostetler product (and our own analysis) found significant wet biases compared to observations for regions near the Wyoming basin (Dominique Bachelet, Conservation Biology Institute, oral commun.). The Hostetler product also divides the west into four “tiles,” or downscaling regions, and Wyoming is included in all of them but with different results depending on the tile (not shown). The advantages of the dynamically downscaled product is that it may better represent dynamics and includes useful hydrologic variables (available for BCSO, but not for the Rehfeldt product), the issues with the different tiles and large wet bias introduced complexities that were beyond original scope and budget of this project. For these reasons, and especially because of the opportunity to take advantage of ecological studies already published in the peer review literature, we chose to work primarily with other downscaled products.

The BCSO product has been used for planning and policy purposes by the Bureau of Reclamation (Bureau of Reclamation 2011, 2013), and is being widely used in hydrologic and ecological studies. Although it is subject to some of the same critiques as other statistical products (for example, that it does not reflect changes in dynamic patterns, or extremes outside the recent range), it is a reasonable choice for evaluating future risks at the level of biomes.

The Rehfeldt product is the basis for a large body of work relevant to the REA, but it has been used primarily by Rehfeldt and his coworkers and Wyoming BLM wanted to know whether it was a reasonable choice. The Rehfeldt and Hostetler products did not downscale any of the same GCMs, and thus were not easy to compare. Maurer and Rehfeldt downscalings are very similar for temperature and precipitation for several GCMs we looked at that both products downscaled, which is not surprising given that they have similar statistical downscaling methodologies. Figure A–14 shows their results for temperature for the GFDL2.1 model.

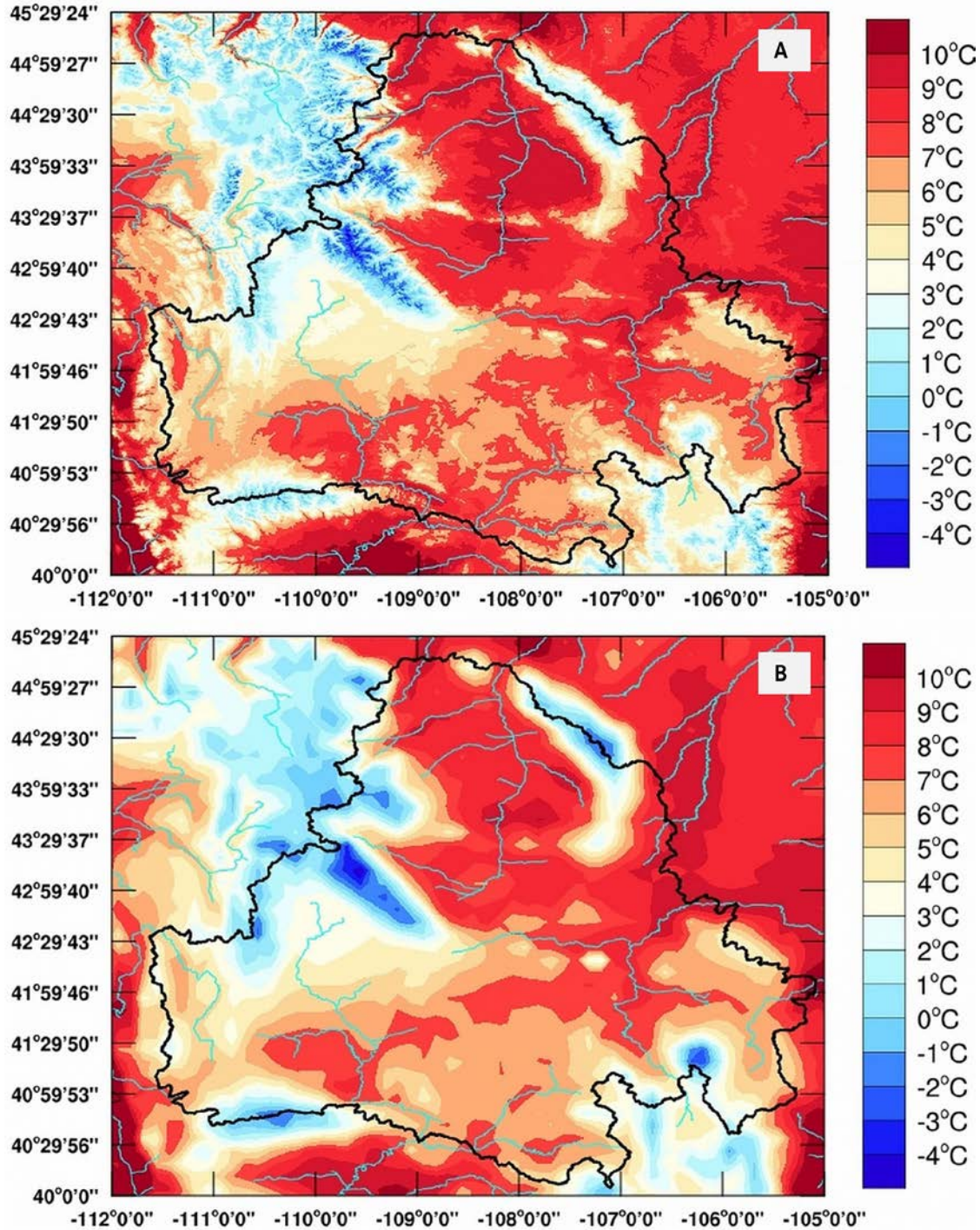


Figure A-14. Annual average temperature around 2030 shown for downscaled products at two resolutions. Maps illustrate the difference in resolution of the (A) 1-km (0.62-mi) Rehfeldt product and (B) the 12-km (7.46-mi) BCSD products for the same global climate model, National Oceanic and Atmospheric Administration Geophysical Fluid Dynamics Laboratory Climate Model, version 2.1 (GFDL2.1). The two statistical methodologies are very similar as expected because of the similar methods; the main difference is the finer scale of the Rehfeldt product.

We think that the smaller spatial scale Rehfeldt product (1 km [0.6 mi]) is appropriate for the modeling of aspen and other trees in mountainous areas, because changes in temperature with elevation (lapse rate) are likely to be significant over small distances in the mountainous terrain of the tree species of concern. Even given that the smoothing involved in the thin spline technique, the 1-km (0.62-mi) downscaling product may provide an improved finer scale for the elevation differences that would be relevant for those Conservation Elements, compared to the 4-km (2.49-mi) BCSD. There is a trade-off, however, between the downscaling providing value-added information and giving a false sense of increased accuracy. The “added value” information in the finer-resolution downscaling is the elevation, slope, and aspect derived from the digital elevation model. Therefore, for most analyses, we believe that 12-km (7.46-mi) BCSD is as small a resolution as is reasonable. Furthermore, the BCSD product (and the related Western Streamflow dataset) includes hydroclimate variables not available in the Rehfeldt product. In our judgment, the larger resolution of the BCSD product is reasonable for the biome scale of interest for this REA analysis. We have used the BCSD downscaling for most of the analysis and graphics discussed in the Chapter 7— Climate. Its use means we can be consistent across the various plots for temperature, precipitation, and hydroclimate variables like soil moisture and streamflow. For most of Chapter 7— Climate Analysis, we discuss and use maps using the BCSD downscaling (for example, figs. 7–6 to 7–8, 7–10, 7–12). Figure 7–9 also uses the BCSD downscaling but is from an analysis done for Ray and others (2008).

A concern with using a downscaling product that has only a few GCMs is that it represents only a small number of reasonably foreseeable futures. We consider a range of GCMs downscaled in order to represent a range of reasonably foreseeable futures, and we use graphics and analysis like that in figure 7–5 and discussed further below, to understand how individual models compare to each other and to the range of climates in a larger ensemble of GCMs. This process is described further in the section below.

Visualizing the Climates in the Downscaled Global Climate Models

A major challenge for the overall REA is that each of these products downscaled a different set of GCMs (see table A–22): Hostetler downscaled one run each from ECHAM5, GFDL2.0, and GENMOM driven by the A2 emissions scenario; Rehfeldt downscaled GFDL2.1, HADCM3, and CCCM3 driven by the A2 scenario; the Western Streamflow Database downscaled PCM1 and MIROC, driven by the A1B scenario; and the Maurer BCSD includes all of these except GENMOM in a suite of 16 CMIP3 GCMs, and includes B2, A1B, and the A2 emissions scenarios. This could have implications for evaluating the results of different ecological studies that used different downscaling products, with the potential for results of the studies to be misinterpreted. For examples, differences in GCMs and other downscaling methods resulted in very different projected bioclimatic envelopes for sagebrush steppe (Rehfeldt and others, 2012; Schlaepfer and others, 2011).

For the analysis and graphics in Chapter 7—Climate, we focused on the GCMs downscaled by Hostetler (ECHAM5 and GFDL2.0) and Rehfeldt (GFDL2.1, HADCM3, and CCCM3) and then show how the climate in those GCMs relates to the larger set of models downscaled by Maurer. Graphics in Chapter 7—Climate Analysis bracket three reasonably foreseeable futures: GFDL 2.1 shows an increase in precipitation and a relatively larger increase in temperature; the 36-member ensemble average shows little change in precipitation; and ECHAM5 shows a small decrease in precipitation and a relatively smaller increase in temperature.

A simple way to put the various GCMs in context to each other is to plot the temperature versus precipitation for particular places, because the climate in different downscaling products depends greatly on the climate they “inherit” from the driving GCM. In other words, what different climate futures did they show, and how did they relate to each other (that is, is the GCM or run selected

warmer/cooler/drier in the range of many GCMs?). We plotted the output of the downscaled GCMs that we focused on in this report by using the BCSD product which downscaled 16 GCMs including all of those downscaled by Hostetler, Rehfeldt, and the Western Streamflow Database. Because the BCSD creators excluded the least performing GCMs and kept 16 GCMs, we consider that the whole scatterplot distribution represents reasonably foreseeable futures, for 2030 and 2060, as described in Chapter 7—Climate Analysis.

Figures A–15 and 7–5 show scatterplots of the projected temperature versus precipitation for all the models (including several ensemble members, or runs, of the same model) for the central valley area and a representative mountain area, the Wind River Range. These figures allow us characterize the range of climate futures in the different GCMs and the climates in specific GCMs.

- ECHAM5 projects a future that is slightly cooler (~ 0.2 °C) than the ensemble mean and with a slight precipitation decrease in the later period that is within the natural variability.
- GFDL2.0 and GFDL2.1 (a newer version of the same model) project quite different futures for 2016–2030 with GFDL2.0 drier than the ensemble mean and GFDL2.1 wetter and also ~ 0.4 °C warmer.
- CCCM3 and HADCM3 are very similar to the ensemble mean for 2016–2030 and project a future wetter than the ensemble for the 2046–2060 period.
- PCM1 and MIROC runs driven by the A1B scenario (unlike all the others in this figure, which were driven by the A2 scenario) were selected by the creators of the Western U.S. Streamflow Metric Dataset as representative ends of a temp-precipitation range, with MIROC projecting a “warmer and drier summers than the ensemble mean,” and PCM1, projecting “cooler and wetter summers than the ensemble mean.” For the Wyoming Basin, however, although PCM1 is cooler and wetter than the ensemble, MIROC is warmer but also wet and slightly dry for 2046–2060.

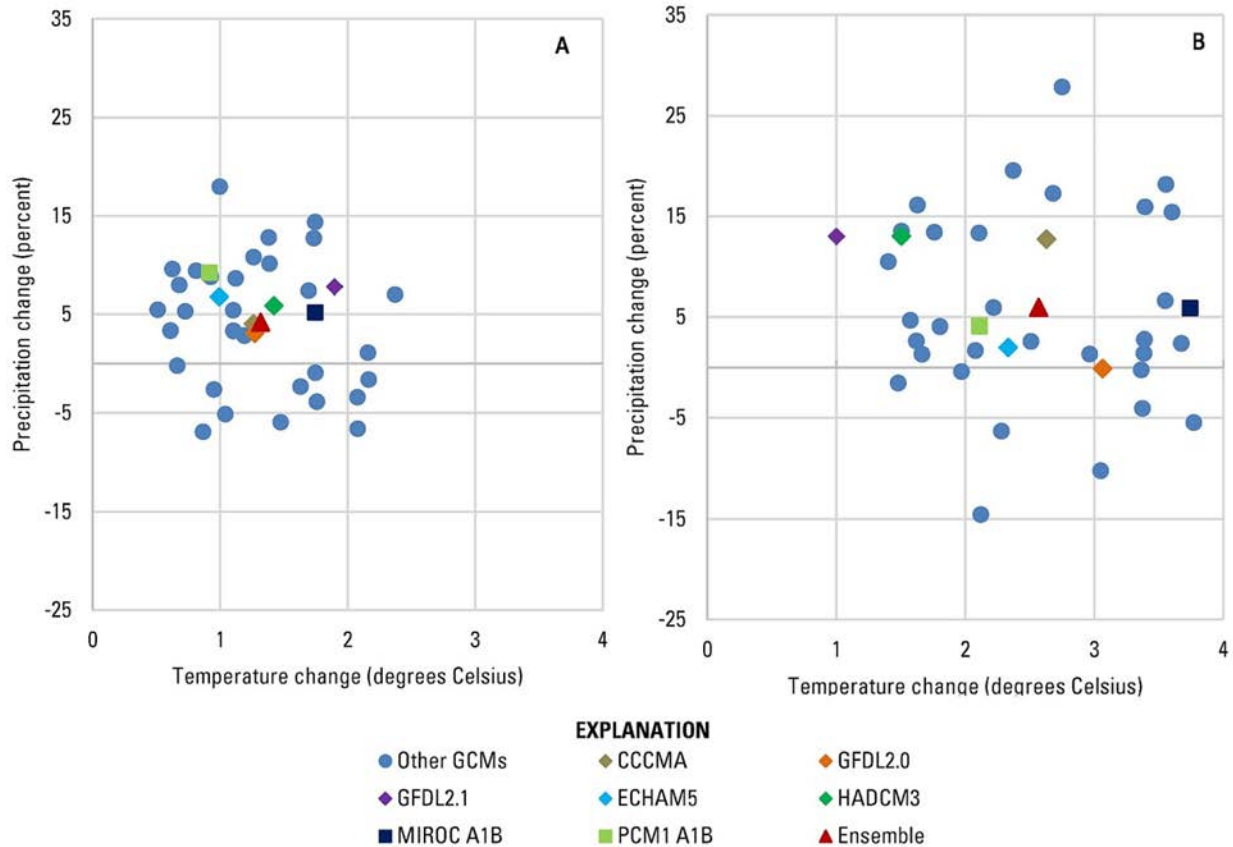


Figure A-15. Range of projected futures in global climate models (GCMs) for the Wind River Range. Annual temperature and precipitation changes between the current climate (1961–1990) and (A) 2016–2030 and (B) 2046–2060 downscaled for the Wind River Range, a representative mountain area, show the range of futures in 16 GCMs downscaled by BCSD. These plots show that the cloud of model results is warmer in the latter period and reveal the climates in the models; for example, the Canadian Centre for Climate Modeling and Analysis Coupled Global Model, version 3 [CCCMA] and the Hadley Centre Coupled Model, version 3 [HADCM3] are very similar to each other; the ensemble mean for 2016–2030 and the National Oceanic and Atmospheric Administration Geophysical Fluid Dynamics Laboratory Climate Model, version 2.1 [GFDL2.1] has a climate that is both warmer and wetter than most of the other GCMs. There are multiple runs of some GCMs for 36 total runs. Downscaled GCMs used in this report are labelled on the graph, including the European Center Hamburg Model, version 5 (ECHAM5), National Oceanic and Atmospheric Administration Geophysical Fluid Dynamics Laboratory Climate Model, version 2.0 (GFDL2.0) GFDL2.1, CCCMA, and HADCM3, and the 36-member ensemble mean were all forced by the A2 emissions scenario. PCM1 and MIROC (blue), which are part of the Western U.S. Streamflow Metric Dataset, which were forced by the A1B scenario. The long term (1895–2013) 1-standard deviation in annual precipitation for this area is about +/-5 percent. BCSD data, 12-km (7.5-mi) resolution.

The seven GCMs used in the suite of GCM's downscaled by Hostetler, Rehfeldt, and Littell are within the "cloud" of reasonably foreseeable futures in the larger suite of GCMs downscaled by BCSO, although they represent a smaller range of futures than the BCSO ensemble. Most of the plots and graphics in this report will display downscaling of ECHAM5, dynamically downscaled by Hostetler and statistically downscaled by BCSO and GFDL2.1, and the ensemble mean of 36 runs of 9 GCMs show the climate the different GCMs project (scatterplot). ECHAM5 shows a relatively cooler/less warming 2030, but catches up by mid-century; HADCM3 and CCCMA models statistically downscaled by Rehfeldt and Maurer are similar. ECHAM5 (downscaled by Hostetler) is similar in temperature and precipitation change compared to HADCM3 and CCCMA (downscaled by Rehfeldt); GFDL 2.0 (downscaled by Hostetler) is slightly cooler than GFDL2.1 (downscaled by Rehfeldt) but similar in precipitation.

Hydroclimate

Figures 7–14 to 7–16 in Chapter 7—Climate Analysis show two views of projected soil moisture change. Figure 7–14 shows a time series of soil moisture for six GCMs focused on in this report (CCCMA3, GFDL2.0 and 2.1, ECHAM5, HADCM3, GCM MIROC, and PCM1) and for the 36-member ensemble average. The time series, beginning with simulated soil moisture from 1950, shows projections to 2099 with a slight downward trend for the lower elevation area near Baggs, Wyo., and a larger trend for an area near Lizardhead Peak in the Wind River Mountains. These figures also show variability of approximately ± 10 percent, depending on the GCM.

Figures 7–15 and 7–16 then illustrate the month to month changes in soil moisture that may occur over the next 100 years and show seasonal shifts in soil moisture that may have ecological consequences. To understand the changes, we needed to account for the variability in the soil moisture record and projections and for the issue that modeled soil moisture is not directly comparable to observations. Soil moisture variables are essentially an index of the moisture state in the soil (Koster and others, 2009) but can be considered as a relative measure of changes. We analyzed the projected changes of relative changes normalized to the variability in the 1961–1990 period analyzed for this report. For each of six GCMs and the 36-member ensemble mean, we calculated the monthly mean soil moisture for the 1961–1990 climate; then, we calculated normalized soil moisture for two future periods for each model and the ensemble mean. The resulting plots by month for two areas show the projected seasonal shift in soil moisture. Recall from figure 7–5 that the climate of the ensemble mean has an increase in temperature and little change in annual precipitation, although, as shown in figure 7–13, there is an increase in winter precipitation and a decrease in summer precipitation. Figure 7–15A shows that the effect of this temperature increase is to decrease soil moisture in the late summer and fall but with an increase in the winter, probably resulting from the increased winter precipitation. Figure 7–15B shows the same area around Baggs, Wyo., but for the GFDL2.1 GCM, which is warmer and wetter than the ensemble (see figure 7–5). The implications of the wetter future are that the temperature impact is nearly offset in the early part of the year by increased winter precipitation, but summer precipitation is also projected to be lower, and as a result, soils are projected to dry out earlier in the summer and the fall. Figure 7–16B shows the same analysis for an area near Lizardhead Peak in the Wind River Range.

Data Gaps and Uncertainty

Regional and national datasets, such as LANDFIRE, TIGER, National Wetlands Inventory, and National Hydrography Dataset, often have spatial inaccuracies that limit their use at scales approaching the resolution of the datasets (such as 30 m for LANDFIRE) but such spatial inaccuracies can be

minimized using moving windows (such as the TDI). Many datasets were compiled from the five states within the ecoregion, and differences across state boundaries can result from underlying differences in the state-level data. Some datasets available for the ecoregion, such as water diversion data, varied spatially in completeness. In many cases, available regional-level data on Change Agents were not sufficient for use in the REA. This included grazing levels, off-highway vehicle use, traffic levels, invasive species occurrence, beaver occurrence/beaver ponds, and fire occurrence and severity (prior to 1980). This limited our ability to fully evaluate the degree of human modification of the landscape, and instead we focused the REA assessment framework on the surface disturbance footprint for development variables. In addition, we lack information on how most species respond to development levels, and the level of development at which the species responds negatively to development (for example, $TDI > 3$ or $TDI > 5$) varies among species. Consequently, risk from development is best viewed as a gradient, with greater confidence in the potential risk from development at either end of the gradient; relatively undeveloped areas have the least risk from development compared to the risk in areas with high levels of development.

Occurrence information on species across the entire ecoregion was sometimes quite limited (especially for most fish species except cutthroat trout), and in some cases, the spatial accuracy of mapped occurrences (such as migration corridors for mule deer) was quite variable within and between states or only were available for certain times of the year (for example, breeding season for greater sage-grouse and crucial winter range for mule deer). In most cases, we had independent datasets to validate the species distribution models (such as greater sage-grouse, sagebrush-obligate songbirds, golden eagles, ferruginous hawks), but in other cases, independent datasets were lacking (for example, spadefoot assemblage).

The REAs summarize broad-scale information that provides the larger context for local management decisions, but often lack the spatial resolution that provides local information on condition. Often, more detailed information is available locally, but it may not be available for broad geographic extents. As a result, both broad- and local-scale information may be necessary to address particular Management Questions. Additionally, the REAs can provide assessments of spatially explicit cumulative effects of Change Agents, especially development. The REAs, therefore, contribute to multiscale information necessary for implementing the BLM's Landscape Approach.

References Cited

- Annis, G.M., Sowa, S.P., Diamond, D.D., Combes, M.D., Doisy, K.E., Garringer, A.J., and Hanberry, P., 2010, Developing synoptic human threat indices for assessing the ecological integrity of freshwater ecosystems in EPA Region 7, final report: Columbia, Mo., University of Missouri, School of Natural Resources, 192 p.
- Barsugli, J.J., Vogel, J.M., Kaatz, Laurina, Smith, J., Waage, Marc, and Anderson, C.J., 2012, Two faces of uncertainty—Climate science and water utility planning: *Journal of Water Resources Planning and Management*, v. 138, no. 5, p. 389–395.
- Beetle, A.A., and Johnson, K.L., 1982, Sagebrush in Wyoming: Laramie, Wyo., Agricultural Experiment Station University of Wyoming, Bulletin no. 779.
- Bureau of Reclamation, 2011, West-wide climate risk assessments—Bias-corrected and spatially downscaled surface water projections: Denver, Colo., Bureau of Reclamation, Technical Service Center, Technical Memorandum 86–68210–2011–01.
- Bureau of Reclamation, 2013, Downscaled CMIP3 and CMIP5 climate and hydrology projections—Release of downscaled CMIP5 climate projections, comparison with preceding information, and

- summary of user needs: Denver, Colo., U.S. Department of the Interior, Bureau of Reclamation, Technical Services Center, 47 p.
- Cayan, Daniel, Tyree, Mary, Kunkel, K.E., Castro, C.L., Gershunov, Alexander, Barsugli, J.J., Ray, A.J., Overpeck, Jonathan, Anderson, Michael, Russell, Joellen, Rajagopalan, Balaji, Rangwala, Imtaz, and Duffy, Paul, 2013, Future climate—Projected average, *in* Garfin, Greg, Jardine, Angela, Merideth, Robert, Black, Mary, and LeRoy, Sarah, eds., Assessment of climate change in the Southwest United States—A report, prepared for the National Climate Assessment: Washington, D.C., Island Press, Southwest Climate Alliance, p. 101–125.
- Chang, E.K.M., Guo, Yanjuan, and Xia, Xiaoming, 2012, CMIP5 multimodel ensemble projection of storm track change under global warming: *Journal of Geophysical Research*, v. 117, D23118.
- Daly, Christopher, Halbleib, Michael, Smith, J.I., Gibson, W.P., Doggett, M.K., Taylor, G.H., Curtis, Jan, and Pasteris, P.A., 2008, Physiographically sensitive mapping of temperature and precipitation across the conterminous United States: *International Journal of Climatology*, v. 28, p. 2031–2064.
- Denholm, Paul, Hand, Maureen, Jackson, Maddalena, and Ong, Sean, 2009, Land-use requirements of modern wind power plants in the United States: Golden, Colo., National Renewable Energy Laboratory, Report NREL/TP–6A2–45834, 39 p.
- Di Luzio, Mauro, Johnson, G.L., Daly, Christopher, Eischeid, J.K., and Arnold, J.G., 2008, Constructing retrospective gridded daily precipitation and temperature datasets for the conterminous United States: *Journal of Applied Meteorology and Climatology*, v. 47, p. 475–497.
- Elith, J., Kearney, M. and Phillips, S., 2010, The art of modelling range-shifting species: *Methods in Ecology and Evolution*, v. 1, p. 330–342.
- Elsner, M.M., Cuo, Lan, Voisin, Nathalie, Deems, J.S., Hamlet, A.F., Vano, J.A., Mickelson, K.E.B., Lee, Se-Yeun, and Lettenmaier, D.P., 2010, Implications of 21st century climate change for the hydrology of Washington State: *Climatic Change*, v. 102, nos. 1–2, p. 225–260.
- Esri, 2011, ArcGIS Desktop—Release 10: Redlands, Calif., Environmental Systems Research Institute.
- Esri Water Resources Team, 2011, Arc Hydro Tools water resource support toolbox, version 2.0: Redlands, Calif. (Available at http://downloads.esri.com/blogs/hydro/ah2/arc_hydro_tools_2_0_overview.pdf.)
- Fowler, H.J., Blenkinsop, Stephen, and Tebaldi, Claudia, 2007, Linking climate change modeling to impacts studies—Recent advances in downscaling techniques for hydrological modeling: *International Journal of Climatology*, v. 27, p. 1547–1578.
- Gershunov, Alexander, Rajagopalan, Balaji, Overpeck, Jonathan, Guirguis, Kristen, Cayan, Daniel, Hughes, Mimi, Dettinger, Michael, Castro, Christopher, Schwartz, R.E., Anderson, Michael, Ray, A.J., Barsugli, J.J., Cavazos, Tereza, and Alexander, M.A., 2013, Future climate—Projected extremes, *in* Garfin, Greg, Jardine, Angela, Merideth, Robert, Black, Mary, and LeRoy, Sarah, eds., Assessment of climate change in the Southwest United States—A report, prepared for the National Climate Assessment: Washington, D.C., Island Press, Southwest Climate Alliance, p. 126–147.
- Hanser, S.E., Leu, M., Knick, S.T., and Aldridge, C.L., eds., 2011, Sagebrush ecosystem conservation and management—Ecoregional assessment tools and models for the Wyoming Basins: Lawrence, Kans., Allen Press, at <http://sagemap.wr.usgs.gov/wbea.aspx>.
- Harggett, E.G., 2011, The Wyoming Stream Integrity Index (WSII)—Multimetric indices for assessment of Wadeable streams and large rivers in Wyoming: Cheyenne, Wyo., Wyoming Department of Environmental Quality, Water Quality Division, 102 p.
- Harggett, E.G., and ZumBerge, J.R., 2006, Redevelopment of the Wyoming Stream Integrity Index (WSII) for assessing the biological condition of Wadeable streams in Wyoming: Cheyenne, Wyo., Wyoming Department of Environmental Quality, Water Quality Division, 777 p.

- Hayhoe, Katharine, Cayan, Daniel, Field, C.B., Frumhoff, P.C., Maurer, E.P., Miller, N.L., Moser, S.C., Schneider, S.H., Cahill, K.N., Cleland, E.E., Dale, Larry, Drapek, Ray, Hanemann, R.M., Kalkstein, L.S., Lenihan, James, Lunch, C.K., Neilson, R.P., Sheridan, S.C., and Verville, J.H., 2004, Emissions pathways, climate change, and impacts on California: Proceedings of the National Academy of Sciences, v. 101, no. 34, p. 12422–12427.
- Hayhoe, Katharine, Wake, C.P., Huntington, T.G., Luo, Lifeng, Schwartz, M.D., Sheffield, Justin, Wood, Eric, Anderson, Bruce, Bradbury, James, DeGaetano, Art, Troy, T.J., and Wolfe, David, 2008, Past and future changes in climate and hydrological indicators in the U.S. Northeast: Climate Dynamics, v. 28, no. 4, p. 381–407.
- Hijmans, R.J., Cameron, S.E., Parra, J.L., Jones, P.G., and Jarvis, A., 2005, Very high resolution interpolated climate surfaces for global land areas: International Journal of Climatology, v. 25, p. 1965–1978.
- Homer, C.G., Aldridge, C.L., Meyer, D.K., and Schell, S.J., 2012, Multi-scale remote sensing sagebrush characterization with regression trees over Wyoming, USA—Laying a foundation for monitoring: International Journal of Applied Earth Observation and Geoinformation, v. 14, p. 233–244.
- Hostetler, S.W., Alder, J.R., and Allan, A.M., 2011, Dynamically downscaled climate simulations over North America—Methods, evaluation, and supporting documentation for users: U.S. Geological Survey Open-File Report 2011–1238, 64 p.
- Intergovernmental Panel on Climate Change, 2013, Climate change 2013—The physical science basis, *in* Stocker, T.F., Qin, Dahe, Plattner, G.-K., Tignor, Melinda, Allen, S. K., Boschung, Judith, Nauels, Alexander, Xia, Yu, Bex, Vincent, and Midgley, P.M., eds., Contribution of Working Group I to the Fifth Assessment Report of the Intergovernmental Panel on Climate Change: Cambridge, United Kingdom, Cambridge University Press.
- Janes, S.W., 1985, Behavioral interactions and habitat relations among grassland and shrub-steppe raptors: Los Angeles, Calif., University of California, Ph. D. dissertation.
- Jarnevich, C.S., and Reynolds, L.V., 2010, Challenges of predicting the potential distribution of a slow-spreading invader—A habitat suitability map for Russian olive (*Elaeagnus angustifolia*) in the western United States: Biological Invasions, v. 13, p. 153–163.
- Jarnevich, C.S., Evangelista, P., Stohlgren, T.J. and Morissette, J., 2011, Improving national-scale invasion maps—Tamarisk in the Western United States: Western North American Naturalist, v. 71, 164–175.
- Jiménez-Valverde, A., Peterson, A.T., Soberón, J., Overton, J.M., Aragón, P. and Lobo, J.M., 2011, Use of niche models in invasive species risk assessments: Biological Invasion, v. 13, p. 2785–2797.
- Karl, T.R., Meehl, G.A., Miller, C.D., Hassol, S.J., Waple, A.M., and Murray, W.L., eds, 2008, Regions of Focus—North America, Hawaii, Caribbean, and U.S. Pacific Islands, *in* 3.3 Weather and climate extremes in a changing climate, A report by the U.S. Climate Change Science Program and the Subcommittee on Global Change Research: Washington, D.C., Department of Commerce, National Oceanic and Atmospheric Administration, National Climatic Data Center, 164 p. (Available at <http://downloads.globalchange.gov/sap/sap3-3/sap3-3-final-all.pdf>.)
- Katzner, T.E., and Parker, K.L., 1997, Vegetative characteristics and size of home ranges used by pygmy rabbits (*Brachylagus idahoensis*) during winter: Journal of Mammalogy, v. 78, p. 1063–1072.
- Knick, S.T., Hanser, S.E., and Preston, K.L., 2013, Modeling ecological minimum requirements for distribution of greater sage-grouse leks—Implications for population connectivity across their western range, USA: Ecology and Evolution, v. 3, no. 6, p. 1539–1551.
- Knight, D.H., 1994, Mountains and plains—The ecology of Wyoming landscapes: New Haven, Conn., Yale University Press, 338 p.

- Knutti, Reto, and Sedláček, Jan, 2013, Robustness and uncertainties in the new CMIP5 climate model projections: *Nature Climate Change*, v. 3, p. 369–373, doi:10.1038/nclimate1716.
- Koster, R.D., Guo, Zhichang, Dirmeyer, P.A., Yang, Ronqian, Mitchell, Kenneth, and Puma, M.J., 2009, On the nature of soil moisture in land surface models: *Journal of Climate*, v. 22, p. 4322–4335, doi:10.1175/2009JCLI2832.1.
- Kunkel, K.E., Stevens, L.E., Stevens, S.E., Sun, Liqiang, Janssen, Emily, Wuebbles, Donald, Kruk, M.C., Thomas, D.P., Shilski, M.D., Umphlett, N.A., Hubbard, K.G., Robbins, K., Romolo, Luigi, Akuz, Adnan, Pathak, T.B., Bergantino, T.R., and Dobson, J.G., 2013, *Climate of the U.S.—Great Plains: National Oceanic and Atmospheric Administration Technical Report NESDIS 142–4*. [Available at http://www.hprcc.unl.edu/publications/files/NOAA_NESDIS_Tech_Report_142-4-Climate_of_the_U.S.%20Great_Plains.pdf.]
- LANDFIRE, 2010, Existing Vegetation Type—Refresh 2008: U.S. Geological Survey, Wildland Fire Science, Earth Resources Observation and Science Center, <http://www.landfire.gov/>.
- Littell, J.S., and Gwozdz, R.B., 2011, Climatic water balance and regional fire years in the Pacific Northwest, USA—Linking regional climate and fire at landscape scales, *in* McKenzie, D.M., Miller, C.M., and Falk, D.A., eds., *The landscape ecology of fire*: Dordrecht, The Netherlands, Springer, *Ecological Studies* 213, p. 117–139.
- Littell, J.S., Elsner, M.M., Mauger, G.S., Lutz, E.R., Hamlet, A.F., and Salathé, E.P., 2011, Regional climate and hydrologic change in the Northern U.S. Rockies and Pacific Northwest—Internally consistent projections of future climate for resource management: Seattle, Wash., University of Washington, Climate Impacts Group, at http://ces.washington.edu/picea/USFS/pub/Littell_etal_2010/Littell_etal_2011_Regional_Climatic_And_Hydrologic_Change_USFS_USFWS_JVA_17Apr11.pdf, accessed April 10, 2014.
- Littell, J.S., McKenzie, D.M., Peterson, D.L., and Westerling, A.J., 2009, Climate and wildfire area burned in western U.S. ecoregions, 1916–2003: *Ecological Applications*, v. 19, no. 4, p. 1003–1021.
- Littell, J.S., Oneil, E.E., McKenzie, D.M., Hicke, J.A., Lutz, J.A., Norheim, R.A., and Elsner, M.M., 2010, Forest ecosystems, disturbance, and climatic change in Washington State, USA: *Climatic Change*, v. 102, p. 129–158.
- Lukas, Jeff, Barsugli, J.J., Doesken, Nolan, Rangwala, Imtiaz, and Wolter, Klaus, 2014, *Climate change in Colorado—A synthesis to support water resources management and adaptation*: Boulder, Colo., University of Colorado, by the Western Water Assessment for the Colorado Water Conservation Board, 108 p. [Available at <http://cwcb.state.co.us/environment/climate-change/Pages/main.aspx>.]
- Maurer, E.P., Brekke, Levi, Pruitt, Thomas, and Duffy, P.B., 2007, Fine-resolution climate projections enhance regional climate change impact studies: *Eos, Transactions American Geophysical Union*: v. 88, no. 47, p. 504.
- Morisette, J.T., Jarnevich, C.S., Holcombe, T.R., Talbert, C.B., Ignizio, D., Talbert, M.K., Silva, C., Koop, D., Swanson, A., and Young, N.E., 2013, VisTrails SAHM—Visualization and workflow management for species habitat modeling: *Ecography*, v. 36, p. 129–135.
- National Hydrography Dataset, 2012, NHD (1:24,000k): U.S. Geological Survey Web page, <http://nhd.usgs.gov/index.html>.
- National Transportation Atlas, 2011, Railroad lines data, at <https://catalog.data.gov/dataset/national-transportation-atlas-database-railroads-2011>.
- O'Donnell, M.S., and Fancher, T.S., 2014, Spatial mapping and attribution of Wyoming wind turbines-2012: U.S. Geological Survey, Data Series 828. (Available at <http://dx.doi.org/10.3133/ds828>.)

- O'Donnell, M.S., and Ignizio, D.A., 2012, Bioclimatic predictors for supporting ecological applications in the conterminous United States: U.S. Geological Survey Data Series 691. (Available at <http://pubs.usgs.gov/ds/691/>.)
- O'Donnell, M.S., Fancher, T.S., Freeman, A.T., Ziegler, A.E., Bowen, Z.H., and Aldridge, C.L., 2014, Large-scale Wyoming transportation data—A resource planning tool: U.S. Geological Survey Data Series 821, 21 p. (Available at <http://dx.doi.org/10.3133/ds821>.)
- Paukert, C.P., Pitts, K.L., Whittier, J.B., and Olden, J.D., 2011, Development and assessment of a landscape-scale ecological threat index for the lower Colorado River Basin: *Ecological Indicators*, v. 11, no. 2, p. 304–310.
- Phillips, S.J., Anderson, R.P., and Schapire, R.E., 2006, Maximum entropy modeling of species geographic distributions: *Ecological Modelling*, v. 190, p. 231–259.
- Ray, A.J., Barsugli, J.J., Averyt, K.B., Wolter, K., and Doesken, Nolan, 2008, Colorado climate change—A synthesis to support water resource management and adaptation, a report for the Colorado Water Conservation Board by the NOAA-CU Western Water Assessment: Boulder, Colo, University of Colorado. [Available at <http://cwcb.state.co.us/environment/climate-change/Pages/main.aspx>.]
- Rehfeldt, G.E., Crookston, N.L., Saenz-Romero, Cuauhtemoc, and Campbell, E.M., 2012, North American vegetation model for land-use planning in a changing climate—A solution to large classification problems: *Ecological Applications*, v. 22, no. 1, p. 119–141.
- Rehfeldt, G.E., Crookston, N.L., Warwell, M.V., and Evans, J.S., 2006, Empirical analyses of plant-climate relationships for the western United States: *International Journal of Plant Science*, v. 167, no. 6, p. 1123–1150.
- Rehfeldt, G.E., Ferguson, D.E., and Crookston, N.L., 2009, Aspen, climate, and sudden decline in western USA: *Forest Ecology and Management*, v. 258, p. 2353–2364.
- Rocky Mountain Bird Observatory, 2013, The Rocky Mountain avian data center: Brighton, Colo., Rocky Mountain Bird Observatory, at <http://adc.rmbo.org>, accessed November 26, 2013.
- Roubicek, A.J., Vanderwal, J., Beaumont, L.J., Pitman, A.J., Wilson, P. and Hughes, L., 2010, Does the choice of climate baseline matter in ecological niche modelling?: *Ecological Modelling*, v. 221, p. 2280–2286.
- Schlaepfer, D.R., Lauenroth, W.K., and Bradford, J.B., 2012, Effects of ecohydrological variables on current and future ranges, local suitability patterns, and model accuracy in big sagebrush: *Ecography*, v. 35, p. 374–384.
- SciPy, 2013, Open Source scientific tools for Python, version SciPy-0.7.2, at <http://www.scipy.org/doc/scipy-0.14.0/reference/release.0.7.2.html>.
- Seager, Richard, Ting, Mingfang, Li, Cuihua, Naik, Naomi, Cook, Ben, Nakamura, Jennifer, and Liu, Haibo, 2012, Projections of declining surface-water availability for the southwestern United States, *Nature: Climate Change*, v. 3, p. 482–486.
- Sheffield, Justin, Barrett, A.P., Colle, Brian, Fernando, D.N., Fu, Rong, Geil, K.L., Hu, Qi, Kinter, Jim, Kumar, Sanjiv, Langenbrunner, Baird, Lombardo, Kelly, Long, L.N., Maloney, Eric, Mariotti, Annarita, Meyerson, J.E., Mo, K.C., Neelin, J.D., Nigam, Sumant, Pan, Zaitao, Ren, Tong, Ruiz-Barradas, Alfredo, Serra, Y.L., Seth, Anji, Thibeault, J.M., Stroeve, J.C., Yang, Ze, and Yin, Lei, 2013, North American climate in CMIP5 experiments, part I—Evaluation of historical simulations of continental and regional climatology: *Journal of Climate*, v. 26, no. 23, p. 9209–9245.
- Smith, D.G., and Murphy, J.R., 1973, Breeding ecology of raptors in the eastern Great Basin of Utah: *Brigham Young University Science Bulletin*, v. 13, p. 1–76.
- Theobald, D.M., 2013, A general model to quantify ecological integrity for landscape assessments and US application: *Landscape Ecology*, v. 28, p. 1859–1874.

U.S. Geological Survey, 2012, Mineral resources online spatial data: U.S. Geological Survey Mineral Resources data system, <http://mrdata.usgs.gov/mrds/select.php>.

Walsh, John, Wuebbles, Donald, Hayhoe, Katherine, Kossin, James, Kunkel, Kenneth, Stephens, Graeme, Thorne, Peter, Vose, Russell, Wehner, Michael, Willis, Josh, Anderson, David, Feely, R., Hennon, P., Kharin, V., Knutson, Thomas, Landerer, Felix, Lenton, Thomas, Kennedy, John, and Somerville, Richard, 2014, Our changing climate, *in* Melillo, J.M., Richmond, T.C., and Yohe, G.W., eds., Climate change impacts in the United States—The Third National Climate Assessment: U.S. Global Change Research Program, p. 19-67.